

Master integrals for the NNLO virtual corrections to μe scattering in QED: the planar graphs

Pierpaolo Mastrolia,^{a,b} Massimo Passera,^b Amedeo Primo^{a,b} and Ulrich Schubert^c

^a*Dipartimento di Fisica ed Astronomia, Università di Padova,
Via Marzolo 8, 35131 Padova, Italy*

^b*INFN — Sezione di Padova,
Via Marzolo 8, 35131 Padova, Italy*

^c*High Energy Physics Division, Argonne National Laboratory,
Argonne, IL 60439, U.S.A.*

E-mail: pierpaolo.mastrolia@pd.infn.it, massimo.passera@pd.infn.it,
amedeo.primo@pd.infn.it, schubertmielnik@anl.gov

ABSTRACT: We evaluate the master integrals for the two-loop, planar box-diagrams contributing to the elastic scattering of muons and electrons at next-to-next-to leading-order in QED. We adopt the method of differential equations and the Magnus exponential series to determine a canonical set of integrals, finally expressed as a Taylor series around four space-time dimensions, with coefficients written as combination of generalised polylogarithms. The electron is treated as massless, while we retain full dependence on the muon mass. The considered integrals are also relevant for crossing-related processes, such as di-muon production at e^+e^- -colliders, as well as for the QCD corrections to *top*-pair production at hadron colliders.

KEYWORDS: NLO Computations

ARXIV EPRINT: [1709.07435](https://arxiv.org/abs/1709.07435)

Contents

1	Introduction	1
2	LO cross section and NLO QED corrections	3
3	Four-point topologies	4
4	System of differential equations	5
4.1	Constant GPLs	7
5	One-loop master integrals	8
6	Two-loop master integrals	10
6.1	The first integral family	10
6.2	The second integral family	14
7	Towards the non-planar integrals	16
7.1	Master integrals for the non-planar vertex	16
8	Conclusions	22
A	Auxiliary integrals	23
B	$d\log$-forms	27
B.1	First integral family	27
B.2	Second integral family	31

1 Introduction

The elastic scattering of muons and electrons is one of the simplest and cleanest processes in particle physics. In spite of this simplicity, μe scattering measurements are scarce. In the 60s, experiments at CERN and Brookhaven measured this scattering cross section using accelerator-produced muons [1–4]. At the same time, μe collisions were measured by cosmic-ray experiments [5–8]. The scattering of muons off polarized electrons was then proposed as a polarimeter for high-energy muon beams in the late 80s [9] and measured by the SMC collaboration at CERN a few years later [10].

Recently, a new experiment, MUonE, has been proposed at CERN to measure the differential cross section of the elastic scattering of high-energy muons on atomic electrons as a function of the spacelike (negative) squared momentum transfer [11]. This measurement will provide the running of the effective electromagnetic coupling in the spacelike region

and, as a result, a new and independent determination of the leading hadronic contribution to the muon $g-2$ [11, 12]. In order for this new determination to be competitive with the present dispersive one, which is obtained via timelike data, the μe differential cross section must be measured with statistical and systematic uncertainties of the order of 10ppm. This high experimental precision demands an analogous accuracy in the theoretical prediction.

Until recently, the process $\mu e \rightarrow \mu e$ had received little attention also on the theory side. The few existing theoretical studies mainly focused on its QED corrections at next-to-leading order (NLO) [13–19] and tests of the Standard Model (SM) [20–22]. The QED corrections at next-to-next-to-leading order (NNLO), crucial to interpret the high-precision data of future experiments like MUonE, are not known, although some of the two-loop corrections which were computed for Bhabha scattering in QED [23, 24], for the heavy-to-light quark decay [25–29] and the $t\bar{t}$ production [30–33] in QCD can be applied to elastic μe scattering as well.

In this work we take a first step towards the calculation of the full NNLO QED corrections to μe scattering. In particular, we consider the evaluation of the master integrals (MIs) occurring in the decomposition of the genuine two-loop $2 \rightarrow 2$ planar box-diagrams, namely all the two-loop four-point topologies for μe scattering except for the crossed double box diagram. Given the small value of the electron mass m_e when compared to the muon one m , we work in the approximation $m_e = 0$. In this case, integration-by-parts identities [34–36] yield the identification of a set of 65 MIs, which we compute analytically by means of the differential equation method [37–39]. Elaborating on recent ideas to simplify the system-solving strategy [40, 41], we choose a set of MIs obeying a system of first-order differential equations (DEQs) in the kinematical variables s/m^2 and t/m^2 which is linear in the space-time dimension d , and, by means of Magnus exponential matrix [41], we derive an equivalent system of equations in *canonical form* [40], where the d -dependence of the associated matrices is factorized from the kinematics. Let us emphasize that the use of Magnus exponential matrix to identify a canonical basis of master integrals turned out to be very effective in the context of multi-loop integrals involving several scales [41–44]. The matrices associated with the canonical systems admit a logarithmic-differential ($d\log$) form, whose entries are rational functions of the kinematics; therefore, the canonical MIs can be cast in a Taylor series around $d = 4$, with coefficients written as combinations of generalised polylogarithms (GPLs) [45–48]. The final determination of the MIs is achieved after imposing the boundary conditions, implemented by requiring the regularity of the solutions at special kinematics points, and by using simpler integrals as independent input.

The analytic expressions of the MIs have been numerically evaluated with the help of GiNaC [49] and were successfully tested against the values provided by the computer code SecDec [50]. The package Reduze [51] has been used throughout the calculations.

It is important to observe that the MIs of the QED corrections to $\mu e \rightarrow \mu e$ scattering are related by crossing to the MIs of the QCD corrections to the $t\bar{t}$ -pair production at hadron colliders. The analytic evaluation of the MIs for the leading-color corrections to $pp \rightarrow t\bar{t}$, due to planar diagrams only, was already considered in refs. [30–33]. They correspond to the MIs appearing in the evaluation of the Feynman graphs associated to the topologies T_i with $i \in \{1, 2, 3, 7, 8, 9, 10\}$ in figure 1, which we (re)compute here indepen-

dently. The MIs for the planar topology T_4 and T_5 , instead, would correspond to the MIs of subleading-color contributions to $t\bar{t}$ -pair production, and were not considered previously.

For certain classes of MIs, like the ones of the processes $\mu e \rightarrow \mu e$ and $pp \rightarrow t\bar{t}$, the choice of the boundary conditions may still constitute a challenging problem. In some cases considered in refs. [30–33], the direct integration of the MIs in special kinematic configurations was addressed by using techniques based on Mellin-Barnes representations [52, 53]. Alternatively, here we exploit either the regularity conditions at pseudo-thresholds or the expression of the integrals at well-behaved kinematic points. The latter might be obtained by solving simpler auxiliary systems of differential equations, hence limiting the use of direct integration only to a simple set of input integrals. Our preliminary studies make us believe that the strategy we adopt for the determination of the considered integrals is not only limited to the planar contributions, but it can be applied to the non-planar graphs as well. In particular, we show its application for the determination of the MIs for the non-planar vertex graph [25–29]. Moreover, due to the similarity of the cases, we are confident that it can be very helpful for completing the analytic evaluation of the MIs needed for the two-loop QCD corrections to $pp \rightarrow t\bar{t}$, which are currently known only numerically [54–58].

The paper is organized as follows. In section 2 we describe the kinematics of μe scattering and we give a brief review of the LO and NLO QED contributions to the cross section. In section 3 we fix our notation and conventions for the four-point topologies. In section 4 we discuss the general features of the systems of differential equations satisfied by the MIs and their general solution in terms of generalised polylogarithms. In section 5 we describe the computation of the one-loop MIs and in section 6 we present the results for the planar two-loop MIs. Finally, in section 7 we compute the MIs for the non-planar two-loop vertex. In section 8 we give our conclusions. The information provided in the text is complemented by two appendices: in appendix A we discuss the computation of the auxiliary integrals which have been used to extract some of the boundary constants and, in appendix B, we give the expressions of the dlog-form of the matrices associated to canonical systems.

The analytic expressions of the considered MIs are given in the ancillary files accompanying the arXiv version of this publication.

2 LO cross section and NLO QED corrections

Let us consider the elastic scattering

$$\mu^+(p_1) + e^-(p_2) \rightarrow e^-(p_3) + \mu^+(p_4), \tag{2.1}$$

and define the Mandelstam variables

$$s = (p_1 + p_2)^2, \quad t = (p_2 - p_3)^2, \quad u = (p_1 - p_3)^2, \tag{2.2}$$

satisfying $s + t + u = 2m^2 + 2m_e^2$, with the physical requirements $s > (m_e + m)^2$, $-\lambda(s, m^2, m_e^2)/s < t < 0$, and $\lambda(x, y, z) = x^2 + y^2 + z^2 - 2xy - 2xz - 2yz$ is the Källén function.

The LO QED prediction for the differential cross section of the scattering in (2.1) is

$$\frac{d\sigma_0}{dt} = -4\pi\alpha^2 \frac{(m^2 + m_e^2)^2 - su + t^2/2}{t^2\lambda(s, m^2, m_e^2)}, \quad (2.3)$$

where α is the fine-structure constant. The NLO QED corrections to this cross section were computed long time ago [13–18] and revisited more recently [19]. As a first check, we recalculated these corrections and found perfect agreement with ref. [19], both for the virtual corrections and the soft photon emissions. We note that some of the pioneering publications, like [14, 16], contain typos or errors, so that they cannot be directly employed.

In the rest of this paper we will work in the approximation of vanishing electron mass, $m_e = 0$, i.e. with the kinematics specified by $p_1^2 = p_4^2 = m^2$ and $p_2^2 = p_3^2 = 0$. The master integrals will be conveniently evaluated in the non-physical region $s < 0$, $t < 0$.

3 Four-point topologies

The main goal of this work is the evaluation of the master integrals (MIs) of the planar two-loop four-point functions contributing to μe scattering, drawn in figure 1. For completeness, we will discuss also the evaluation of the MIs of the one-loop four-point function in figure 2.

We consider ℓ -loop m -denominator Feynman integrals in $d = 4 - 2\epsilon$ dimensions of the type

$$\int \prod_{i=1}^{\ell} \widetilde{d^d k_i} \frac{1}{D_1^{n_1} \dots D_m^{n_m}}, \quad n_i \in \mathbb{Z}. \quad (3.1)$$

In our conventions, the integration measure is defined as

$$\widetilde{d^d k_i} = \frac{d^d k_i}{(2\pi)^d} \left(\frac{i S_\epsilon}{16\pi^2} \right)^{-1} \left(\frac{m^2}{\mu^2} \right)^\epsilon, \quad (3.2)$$

with μ being the 't Hooft scale of dimensional regularization and

$$S_\epsilon = (4\pi)^\epsilon \Gamma(1 + \epsilon). \quad (3.3)$$

We choose the following set of propagators for the relevant planar four-point topologies at one- and two-loop:

- For the one-loop integral family, depicted in figure 2,

$$\begin{aligned} D_1 &= k_1^2 - m^2, & D_2 &= (k_1 + p_1)^2, \\ D_3 &= (k_1 + p_1 + p_2)^2, & D_4 &= (k_1 + p_4)^2. \end{aligned} \quad (3.4)$$

- For the first two-loop integral family, which includes the topologies T_1, T_2, T_3, T_7 and T_8 of figure 1,

$$\begin{aligned} D_1 &= k_1^2 - m^2, & D_2 &= k_2^2 - m^2, & D_3 &= (k_1 + p_1)^2, & D_4 &= (k_2 + p_1)^2, \\ D_5 &= (k_1 + p_1 + p_2)^2, & D_6 &= (k_2 + p_1 + p_2)^2, & D_7 &= (k_1 - k_2)^2, \\ D_8 &= (k_1 + p_4)^2, & D_9 &= (k_2 + p_4)^2. \end{aligned} \quad (3.5)$$

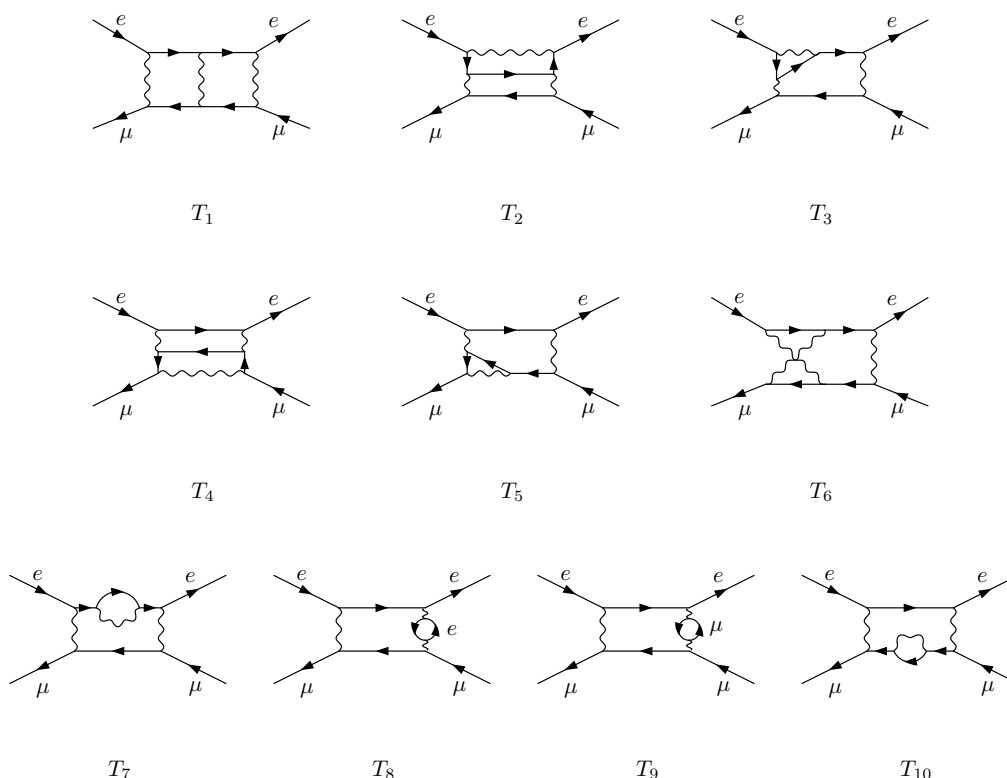


Figure 1. Two-loop four-point topologies for μe scattering.

- For the second two-loop family, which contains topologies T_4 , T_5 , T_9 and T_{10} shown in figure 1,

$$\begin{aligned}
 D_1 &= k_1^2 - m^2, & D_2 &= k_2^2, \\
 D_3 &= (k_2 + p_2)^2, & D_4 &= (k_1 + p_2)^2, \\
 D_5 &= (k_2 + p_2 - p_3)^2, & D_6 &= (k_1 + p_2 - p_3)^2 - m^2, & D_7 &= (k_1 - p_1)^2, \\
 D_8 &= (k_2 - p_1)^2 - m^2, & D_9 &= (k_1 - k_2)^2 - m^2. & & (3.6)
 \end{aligned}$$

For all families, k_1 and k_2 denote the loop momenta. In the following sections, MIs will be represented by diagrams where thick lines stand for massive particles (muon), whereas thin lines stand for massless ones (electron, photon).

4 System of differential equations

In order to determine all MIs appearing in the three integral families defined above, we initially derive their DEQs in the dimensionless variables $-s/m^2$ and $-t/m^2$. Upon the change of variable,

$$-\frac{s}{m^2} = x, \quad -\frac{t}{m^2} = \frac{(1-y)^2}{y}, \quad (4.1)$$

the coefficients of the DEQs are rational functions of x and y . According to our system solving strategy, by means of integration-by-parts identities (IBPs), we choose an initial

set of MIs \mathbf{F} that fulfills a system of DEQs

$$\frac{\partial \mathbf{F}}{\partial x} = \mathbb{A}_x(\epsilon, x, y) \mathbf{F}, \quad \frac{\partial \mathbf{F}}{\partial y} = \mathbb{A}_y(\epsilon, x, y) \mathbf{F}, \quad (4.2)$$

where the matrices $\mathbb{A}_x(\epsilon, x, y)$ and $\mathbb{A}_y(\epsilon, x, y)$ are *linear* in the dimensional regularization parameter $\epsilon = (4 - d)/2$, being d the number of space-time dimensions. According to the algorithm described in [41–44], by means of Magnus exponential matrix, we identify a set of MIs \mathbf{I} obeying canonical systems of DEQs [40], where the dependence on ϵ is factorized from the kinematics,

$$\frac{\partial \mathbf{I}}{\partial x} = \epsilon \hat{\mathbb{A}}_x(x, y) \mathbf{I}, \quad \frac{\partial \mathbf{I}}{\partial y} = \epsilon \hat{\mathbb{A}}_y(x, y) \mathbf{I}. \quad (4.3)$$

After combining both systems of DEQs into a single total differential, we arrive at the following canonical form

$$d\mathbf{I} = \epsilon d\mathbb{A} \mathbf{I}, \quad d\mathbb{A} \equiv \hat{\mathbb{A}}_x dx + \hat{\mathbb{A}}_y dy, \quad (4.4)$$

where the generic form of the total differential matrix for the considered MIs reads as,

$$d\mathbb{A} = \sum_{i=1}^9 \mathbb{M}_i d\log(\eta_i), \quad (4.5)$$

with \mathbb{M}_i being constant matrices. The arguments η_i of this $d\log$ -form, which contain all the dependence of the DEQ on the kinematics, are referred to as the *alphabet* and they consist in the following 9 letters:

$$\begin{aligned} \eta_1 &= x, & \eta_2 &= 1 + x, \\ \eta_3 &= 1 - x, & \eta_4 &= y, \\ \eta_5 &= 1 + y, & \eta_6 &= 1 - y, \\ \eta_7 &= x + y, & \eta_8 &= 1 + xy, \\ \eta_9 &= 1 - y(1 - x - y). \end{aligned} \quad (4.6)$$

Let us observe that, currently, there is neither a proof of existence, nor any systematic algorithm to build a basis of integrals whose system of DEQs is linear in ϵ . Nevertheless, by trial and error, we have been always able to find it within the physical contexts we have so far studied [41–44], as well as for the μe scattering. We believe it is a very important property which could be considered a prerequisite for the existence of a canonical basis: in fact, a system of DEQs whose matrix is linear in ϵ can be brought into canonical form by a rotation matrix built either by means of Magnus exponential, or equivalently by means of the Wronskian matrix (formed by the solutions of the associated homogenous equations, and their derivatives), as shown for the case of systems of DEQs involving elliptic solutions [59–61].

The MIs presented in this paper are computed in the kinematic region where all letters are real and positive,

$$x > 0, \quad 0 < y < 1, \quad (4.7)$$

which corresponds to the Euclidean region $s < 0$, $t < 0$. All MIs are chosen to be finite in the $\epsilon \rightarrow 0$ limit, in such a way that $\mathbf{I}(x, y)$ admits a Taylor expansion in ϵ ,

$$\mathbf{I}(\epsilon, x, y) = \mathbf{I}^{(0)}(x, y) + \epsilon \mathbf{I}^{(1)}(x, y) + \epsilon^2 \mathbf{I}^{(2)}(x, y) + \dots, \quad (4.8)$$

with the n -th order coefficient given by

$$\mathbf{I}^{(n)}(x, y) = \sum_{i=0}^n \Delta^{(n-i)}(x, y; x_0, y_0) \mathbf{I}^{(i)}(x_0, y_0), \quad (4.9)$$

where $\mathbf{I}^{(i)}(x_0, y_0)$ is a vector of boundary constants and $\Delta^{(k)}$ the weight- k operator

$$\Delta^{(k)}(x, y; x_0, y_0) = \int_{\gamma} \underbrace{d\mathbb{A} \dots d\mathbb{A}}_{k \text{ times}}, \quad \Delta^{(0)}(x, y; x_0, y_0) = 1, \quad (4.10)$$

which iterates k ordered integrations of the matrix-valued 1-form $d\mathbb{A}$ along a piecewise-smooth path γ in the xy -plane. Since the alphabet given in eq. (4.6) is rational and has only algebraic roots, the iterated integrals (4.10) can be directly expressed in terms of GPLs, which are defined as

$$G(\vec{w}_n; x) \equiv G(w_1, \vec{w}_{n-1}; x) \equiv \int_0^x dt \frac{1}{t - w_1} G(\vec{w}_{n-1}; t), \quad (4.11)$$

$$G(\vec{0}_n; x) \equiv \frac{1}{n!} \log^n(x), \quad (4.12)$$

with \vec{w}_n being a vector of n arguments. The number n is referred to as the *weight* of $G(\vec{w}_n; x)$ and amounts to the number of iterated integrations needed to define it. Equivalently one has

$$\frac{\partial}{\partial x} G(\vec{w}_n; x) = \frac{\partial}{\partial x} G(w_1, \vec{w}_{n-1}; x) = \frac{1}{x - w_1} G(\vec{w}_{n-1}; x). \quad (4.13)$$

GPLs fulfill shuffle algebra relations of the form

$$G(\vec{m}; x) G(\vec{n}; x) = G(\vec{m}; x) \sqcup \sqcup G(\vec{n}; x) = \sum_{\vec{p} = \vec{m} \sqcup \sqcup \vec{n}} G(\vec{p}; x), \quad (4.14)$$

where the shuffle product $\vec{m} \sqcup \sqcup \vec{n}$ denotes all possible merges of \vec{m} and \vec{n} while preserving their respective orderings.

The analytic continuation of the MIs to the physical region defined in section 2 can be obtained through by-now standard techniques.

4.1 Constant GPLs

Many of the boundary values $\mathbf{I}^{(i)}(x_0, y_0)$ of the MIs have been determined by taking special kinematics limits on the general solution of the DEQs written in terms of GPLs. Through this procedure, the boundary constants are expressed as combinations of constant GPLs of argument 1, with weights drawn from six different sets:

- $\{-1, 0, 1, 3, -(-1)^{\frac{1}{3}}, (-1)^{\frac{2}{3}}\}$,

- $\{-\frac{1}{2}, -\frac{2}{7}, 0, \frac{1}{7}, \frac{1}{2}, \frac{4}{7}, 1, -\frac{1}{2}(-1)^{\frac{1}{3}}, \frac{1}{2}(-1)^{\frac{2}{3}}\},$
- $\{-1, -\frac{1}{2}, 0, \frac{1}{2}, 1, 2, 3, 4, \frac{1}{2}(-1)^{\frac{1}{3}}, -\frac{1}{2}(-1)^{\frac{2}{3}}\},$
- $\{-1, -\frac{1}{2}, 0, \frac{1}{4}, \frac{1}{2}, 1, \frac{7}{4}, \frac{1}{2}(-1)^{\frac{1}{3}}, -\frac{1}{2}(-1)^{\frac{2}{3}}\},$
- $\{-2, -\frac{1}{2}, 0, \frac{1}{2}, 1, 4, 7, -\frac{1}{2}(-1)^{\frac{1}{3}}, \frac{1}{2}(-1)^{\frac{2}{3}}\},$
- $\{-2, -1, -\frac{1}{2}, 0, \frac{1}{4}, 1, \frac{7}{4}, 2, -2(-1)^{\frac{1}{3}}, 2(-1)^{\frac{2}{3}}\}.$

Each set arises from a different kinematic limit imposed on the alphabet given in eq. (4.6). We used GiNaC to numerically verify that at each order in ϵ^n (up to the order $n = 4$), the corresponding combination of constant GPLs is proportional to Riemann ζ_n . In particular, ζ_n functions are known to be *primitive* [62–64], i.e. they have irreducible coproducts, $\Delta(\zeta_n) = 1 \otimes \zeta_n + \zeta_n \otimes 1$. Therefore, they must have vanishing coproducts components $\Delta_p(\zeta_n) = 0$ with $p \in \Pi(n)$, where

$$\begin{aligned} \Pi(n) = \{ & (n-1, 1), (n-2, 2), (n-2, 1, 1), \dots, \\ & \dots, (1, 1, 1, \dots, 1, 1, 1), \dots, (1, 1, n-2), (2, n-2), (1, n-1) \} \end{aligned} \quad (4.15)$$

is the set of the integer partitions of n with dimensions larger than one. We explicitly verified that the combinations of GPLs of argument 1, appearing in the boundary conditions, are also primitive, although the considered coproducts components do not necessarily vanish when acting separately on each GPL involved in those combinations. Therefore, we made a simple *ansatz* that these combinations could be proportional to ζ_n , and we checked it by means of high-precision arithmetic. Below we show some examples for these identities,

$$\begin{aligned} \zeta_2 = & -\frac{1}{2}G(-1; 1)^2 + G(0, -2; 1) + G\left(0, -\frac{1}{2}; 1\right), \quad (4.16) \\ -59\zeta_4 = & \pi^2 \left(G(-1; 1)^2 - 2G(0, -(-1)^{\frac{1}{3}}; 1) - 2G(0, (-1)^{\frac{2}{3}}; 1) \right) - 21\zeta_3 G(-1; 1) \\ & - G(-1; 1)^4 - 18G(0, 0, 0, -(-1)^{\frac{1}{3}}; 1) - 18G(0, 0, 0, (-1)^{\frac{2}{3}}; 1) \\ & + 12G(0, 0, -(-1)^{\frac{1}{3}}, -1; 1) + 12G(0, 0, (-1)^{\frac{2}{3}}, -1; 1) \\ & + 12G(0, -(-1)^{\frac{1}{3}}, -1, -1; 1) + 12G(0, (-1)^{\frac{2}{3}}, -1, -1; 1) + 24G(0, 0, 0, 2; 1). \end{aligned} \quad (4.17)$$

For related studies see also [65–67].

5 One-loop master integrals

In this section we briefly discuss the computation of the master integrals of the one-loop four-point graph shown in figure 2, corresponding to the integral family defined in eq. (3.4). We choose the following set of MIs, which satisfy an ϵ -linear DEQ,

$$F_1 = \epsilon \mathcal{T}_1, \quad F_2 = \epsilon \mathcal{T}_2, \quad F_3 = \epsilon \mathcal{T}_3, \quad F_4 = \epsilon^2 \mathcal{T}_4, \quad F_5 = \epsilon^2 \mathcal{T}_5, \quad (5.1)$$

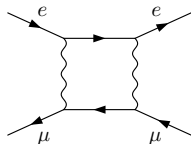


Figure 2. One-loop four-point topology for μe scattering.

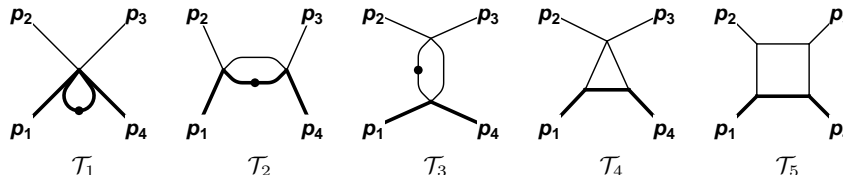


Figure 3. One-loop MIs $\mathcal{T}_{1,\dots,5}$.

where the \mathcal{T}_i are depicted in figure 3. With the help the Magnus algorithm we can identify the corresponding canonical basis

$$\begin{aligned} I_1 &= F_1, & I_2 &= -s F_2, \\ I_3 &= -t F_3, & I_4 &= \lambda_t F_4, \\ I_5 &= (s - m^2)(-t)F_5. \end{aligned} \tag{5.2}$$

with $\lambda_t = \sqrt{-t}\sqrt{4m^2 - t}$.

This set of MIs satisfies a canonical DEQ of the form given in eq. (4.4), whose coefficient matrices read (in this case, \mathbb{M}_3 and \mathbb{M}_9 vanish),

$$\begin{aligned} \mathbb{M}_1 &= \begin{pmatrix} 0 & 0 & 0 & 0 & 0 \\ 0 & 1 & 0 & 0 & 0 \\ 0 & 0 & 0 & 0 & 0 \\ 0 & 0 & 0 & 0 & 0 \\ 0 & 0 & 0 & 0 & 0 \end{pmatrix}, & \mathbb{M}_2 &= \begin{pmatrix} 0 & 0 & 0 & 0 & 0 \\ -1 & -2 & 0 & 0 & 0 \\ 0 & 0 & 0 & 0 & 0 \\ 0 & 0 & 0 & 0 & 0 \\ 2 & 4 & 0 & 0 & -2 \end{pmatrix}, & \mathbb{M}_4 &= \begin{pmatrix} 0 & 0 & 0 & 0 & 0 \\ 0 & 0 & 0 & 0 & 0 \\ 0 & 0 & 1 & 0 & 0 \\ 1 & 0 & -1 & 0 & 0 \\ 1 & 2 & 0 & 0 & 0 \end{pmatrix}, & \mathbb{M}_5 &= \begin{pmatrix} 0 & 0 & 0 & 0 & 0 \\ 0 & 0 & 0 & 0 & 0 \\ 0 & 0 & 0 & 0 & 0 \\ 0 & 0 & 0 & 2 & 0 \\ 0 & 0 & 0 & 0 & 0 \end{pmatrix}, \\ \mathbb{M}_6 &= \begin{pmatrix} 0 & 0 & 0 & 0 & 0 \\ 0 & 0 & 0 & 0 & 0 \\ 0 & 0 & -2 & 0 & 0 \\ 0 & 0 & 0 & -2 & 0 \\ 0 & 0 & 2 & 0 & -2 \end{pmatrix}, & \mathbb{M}_7 &= \begin{pmatrix} 0 & 0 & 0 & 0 & 0 \\ 0 & 0 & 0 & 0 & 0 \\ 0 & 0 & 0 & 0 & 0 \\ 0 & 0 & 0 & 0 & 0 \\ -1 & -2 & -1 & -1 & 1 \end{pmatrix}, & \mathbb{M}_8 &= \begin{pmatrix} 0 & 0 & 0 & 0 & 0 \\ 0 & 0 & 0 & 0 & 0 \\ 0 & 0 & 0 & 0 & 0 \\ 0 & 0 & 0 & 0 & 0 \\ -1 & -2 & -1 & 1 & 1 \end{pmatrix}. \end{aligned} \tag{5.3}$$

The integration of the DEQ in terms of GPLs as well as the fixing of boundary constants is straightforward. $I_{1,3}$ are obtained by direct integration and, by using the normalization of eq. (3.2), are given by

$$I_1(\epsilon) = 1, \quad I_3(\epsilon, y) = \left(\frac{(1-y)^2}{y} \right)^{-\epsilon} (1 - \zeta_2 \epsilon^2 - 2\zeta_3 \epsilon^3 + \mathcal{O}(\epsilon^4)). \tag{5.4}$$

The boundary constants for I_2 , I_4 and I_5 can be fixed by respectively demanding regularity at pseudothresholds $s \rightarrow 0$, at $t \rightarrow 4m^2$, and at $s = -t \rightarrow m^2/2$. The final expression of the other MIs are,

$$I_i(\epsilon, x, y) = \sum_{k=0}^2 I_i^{(k)}(x, y) \epsilon^k + \mathcal{O}(\epsilon^3), \tag{5.5}$$

with

$$\begin{aligned}
 I_2^{(0)}(x) &= 0, \\
 I_2^{(1)}(x) &= -G(-1; x), \\
 I_2^{(2)}(x) &= 2G(-1, -1; x) - G(0, -1; x),
 \end{aligned}
 \tag{5.6}$$

$$\begin{aligned}
 I_4^{(0)}(y) &= 0, \\
 I_4^{(1)}(y) &= 0, \\
 I_4^{(2)}(y) &= -4\zeta_2 - G(0, 0; y) + 2G(0, 1; y),
 \end{aligned}
 \tag{5.7}$$

$$\begin{aligned}
 I_5^{(0)}(x, y) &= 2, \\
 I_5^{(1)}(x, y) &= -2G(-1; x) + G(0; y) - 2G(1; y), \\
 I_5^{(2)}(x, y) &= -5\zeta_2 + 2G(-1; x)(2G(1; y) - G(0; y)).
 \end{aligned}
 \tag{5.8}$$

6 Two-loop master integrals

In this section we present the results for the planar two-loop MIs contributing to the NNLO virtual QED corrections to μe scattering, which are the main results of this work. We first discuss the computation of the MIs belonging to the integral family defined in eq. (3.5), which is associated to the topologies T_1, T_2, T_3, T_7 and T_8 of figure 1, and then the MIs belonging to the integral family defined by eq. (3.6), which groups the topologies T_4, T_5, T_9 and T_{10} .

6.1 The first integral family

For the two-loop family defined in eq. (3.5), the following set of 34 MIs fulfill an ϵ -linear system of DEQs,

$$\begin{aligned}
 F_1 &= \epsilon^2 \mathcal{T}_1, & F_2 &= \epsilon^2 \mathcal{T}_2, & F_3 &= \epsilon^2 \mathcal{T}_3, \\
 F_4 &= \epsilon^2 \mathcal{T}_4, & F_5 &= \epsilon^2 \mathcal{T}_5, & F_6 &= \epsilon^2 \mathcal{T}_6, \\
 F_7 &= \epsilon^2 \mathcal{T}_7, & F_8 &= \epsilon^2 \mathcal{T}_8, & F_9 &= \epsilon^2 \mathcal{T}_9, \\
 F_{10} &= \epsilon^3 \mathcal{T}_{10}, & F_{11} &= \epsilon^3 \mathcal{T}_{11}, & F_{12} &= \epsilon^3 \mathcal{T}_{12}, \\
 F_{13} &= \epsilon^3 \mathcal{T}_{13}, & F_{14} &= \epsilon^2 \mathcal{T}_{14}, & F_{15} &= \epsilon^2 \mathcal{T}_{15}, \\
 F_{16} &= \epsilon^3 \mathcal{T}_{16}, & F_{17} &= \epsilon^4 \mathcal{T}_{17}, & F_{18} &= \epsilon^3 \mathcal{T}_{18}, \\
 F_{19} &= \epsilon^4 \mathcal{T}_{19}, & F_{20} &= \epsilon^2(1 + 2\epsilon) \mathcal{T}_{20}, & F_{21} &= \epsilon^4 \mathcal{T}_{21}, \\
 F_{22} &= \epsilon^3 \mathcal{T}_{22}, & F_{23} &= \epsilon^3 \mathcal{T}_{23}, & F_{24} &= \epsilon^2 \mathcal{T}_{24}, \\
 F_{25} &= \epsilon^3 \mathcal{T}_{25}, & F_{26} &= \epsilon^3(1 - 2\epsilon) \mathcal{T}_{26}, & F_{27} &= \epsilon^3 \mathcal{T}_{27}, \\
 F_{28} &= \epsilon^4 \mathcal{T}_{28}, & F_{29} &= \epsilon^3(1 - 2\epsilon) \mathcal{T}_{29}, & F_{30} &= \epsilon^4 \mathcal{T}_{30}, \\
 F_{31} &= \epsilon^4 \mathcal{T}_{31}, & F_{32} &= \epsilon^4 \mathcal{T}_{32}, & F_{33} &= \epsilon^4 \mathcal{T}_{33}, \\
 F_{34} &= \epsilon^4 \mathcal{T}_{34}, & & & &
 \end{aligned}
 \tag{6.1}$$

where the \mathcal{T}_i are depicted in figure 4.

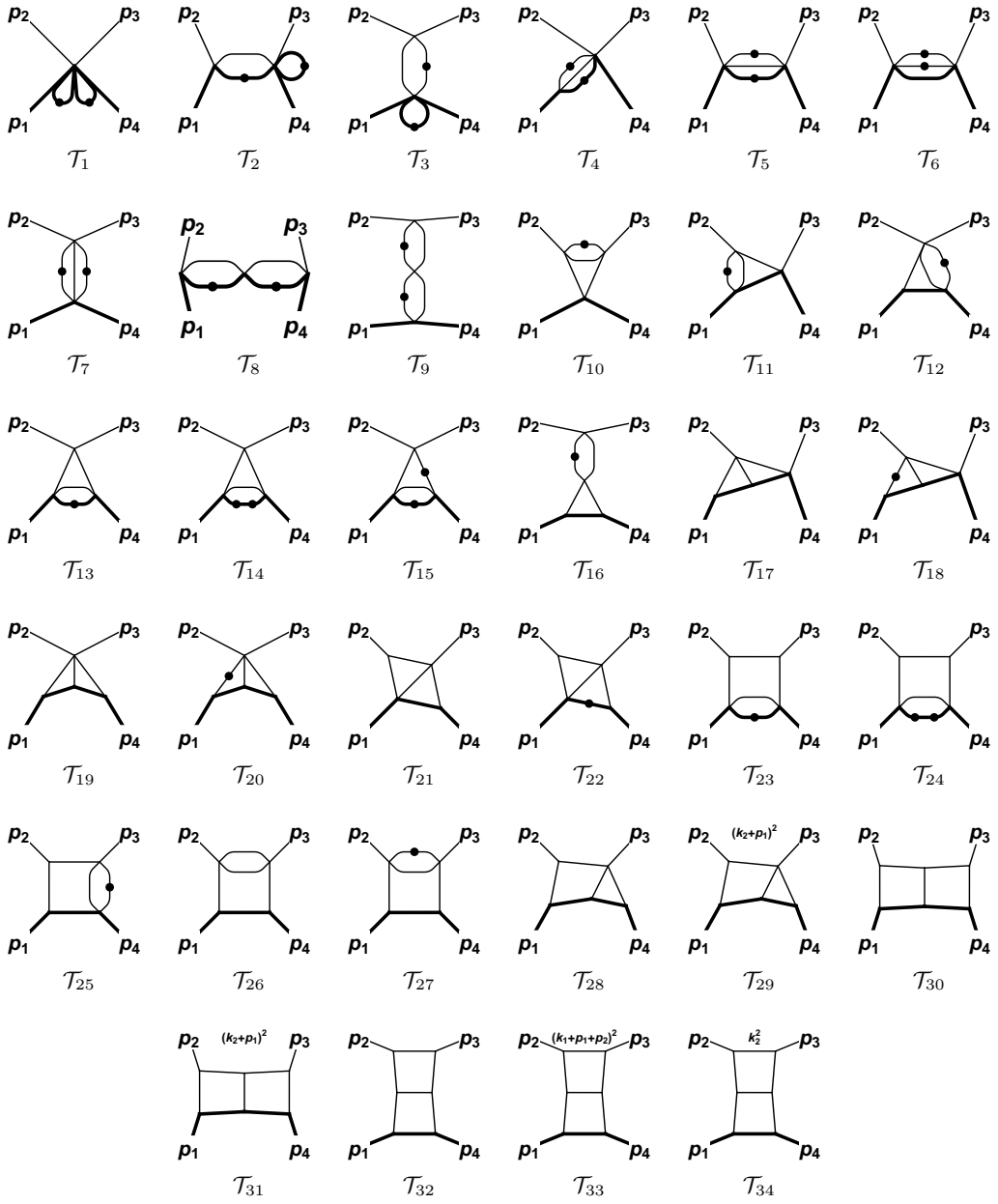


Figure 4. Two-loop MIs $\mathcal{T}_{1,\dots,34}$ for the first integral family.

Through the Magnus exponential, we rotate this set of integrals to the canonical basis

$$\begin{aligned}
 I_1 &= F_1, & I_2 &= -s F_2, \\
 I_3 &= -t F_3, & I_4 &= m^2 F_4, \\
 I_5 &= -s F_5, & I_6 &= 2m^2 F_5 + (m^2 - s) F_6, \\
 I_7 &= -t F_7, & I_8 &= s^2 F_8, \\
 I_9 &= t^2 F_9, & I_{10} &= -t F_{10},
 \end{aligned}$$

$$\begin{aligned}
I_{11} &= (m^2 - s) F_{11}, & I_{12} &= \lambda_t F_{12}, \\
I_{13} &= \lambda_t F_{13}, & I_{14} &= \lambda_t m^2 F_{14}, \\
I_{15} &= (t - \lambda_t) \left(\frac{3}{2} F_{13} + m^2 F_{14} \right) - m^2 t F_{15}, & I_{16} &= -t \lambda_t F_{16}, \\
I_{17} &= (m^2 - s) F_{17}, & I_{18} &= m^2 (m^2 - s) F_{18}, \\
I_{19} &= \lambda_t F_{19}, & I_{20} &= \frac{\lambda_t - t}{2} (F_{12} - 4 F_{19}) - m^2 t F_{20}, \\
I_{21} &= (m^2 - s - t) F_{21}, & I_{22} &= -m^2 t F_{22}, \\
I_{23} &= s t F_{23}, & I_{24} &= -m^2 t F_{23} + (s - m^2) m^2 t F_{24}, \\
I_{25} &= -(m^2 - s) t F_{25}, & I_{26} &= \lambda_t F_{26}, \\
I_{27} &= -(m^2 - s) t F_{27}, & I_{28} &= (m^2 - s) \lambda_t F_{28}, \\
I_{29} &= -2t F_{21} - (m^2 - s)(2(\lambda_t - t)F_{28} - F_{29}), & I_{30} &= -(m^2 - s)^2 t F_{30}, \\
I_{31} &= (m^2 - s)^2 F_{31}, & I_{32} &= (m^2 - s) t^2 F_{32}, \\
I_{33} &= -\lambda_t t F_{33}, & I_{34} &= -m^2 t^2 F_{32} + t^2 F_{34}. \tag{6.2}
\end{aligned}$$

This set of MIs \mathbf{I} satisfies a system of DEQ of the form given in eq. (4.4), which can easily be integrated in terms of GPLs. The 34×34 coefficient matrices are collected in appendix B.1.

To determine the solution of the DEQ, we need to choose proper boundary values for each master integral. The boundary fixing can be achieved either by knowing the integral at some special kinematic point or by demanding the absence of unphysical thresholds that appear in the alphabet of the generic solution, defined in eq. (4.6).

Below we describe in detail how the boundary constants for each integral were chosen:

- The boundary values of $I_{1,3,4,7,9}$ were obtained by direct integration,

$$I_1(\epsilon) = 1, \tag{6.3}$$

$$I_3(\epsilon) = \left(\frac{(1-y)^2}{y} \right)^{-\epsilon} \left(1 - \zeta_2 \epsilon^2 - 2\zeta_3 \epsilon^3 - \frac{9}{4} \zeta_4 \epsilon^4 + \mathcal{O}(\epsilon^5) \right), \tag{6.4}$$

$$I_4(\epsilon) = -\frac{1}{4} - \zeta_2 \epsilon^2 - 2\zeta_3 \epsilon^3 - 16\zeta_4 \epsilon^4 + \mathcal{O}(\epsilon^5), \tag{6.5}$$

$$I_7(\epsilon, y) = \left(\frac{(1-y)^2}{y} \right)^{-2\epsilon} \left(-1 + 2\zeta_2 \epsilon^2 + 10\zeta_3 \epsilon^3 + 11\zeta_4 \epsilon^4 + \mathcal{O}(\epsilon^5) \right), \tag{6.6}$$

$$I_9(\epsilon) = \left(\frac{(1-y)^2}{y} \right)^{-2\epsilon} \left(1 - 2\zeta_2 \epsilon^2 - 4\zeta_3 \epsilon^3 - 2\zeta_4 \epsilon^4 + \mathcal{O}(\epsilon^5) \right), \tag{6.7}$$

$$I_{10}(\epsilon) = \left(\frac{(1-y)^2}{y} \right)^{-2\epsilon} \left(\frac{1}{4} - 2\zeta_3 \epsilon^3 - 3\zeta_4 \epsilon^4 + \mathcal{O}(\epsilon^5) \right). \tag{6.8}$$

- The boundary constants of $I_{2,8,11,23}$ are fixed by demanding finiteness in the limit $s \rightarrow 0$.

- In the regular limit $s \rightarrow 0$, I_5 and I_6 become, respectively,

$$\begin{aligned} I_5(\epsilon, 0) &= 0, \\ I_6(\epsilon, 0) &= \epsilon^2 m^2 (2F_5(\epsilon, 0) + F_6(\epsilon, 0)) . \end{aligned} \quad (6.9)$$

$F_5(\epsilon, 0)$ and $F_6(\epsilon, 0)$ correspond to two-loop vacuum diagrams which can be reduced via IBPs to a single integral which can be analytically computed

$$\begin{aligned} F_5(\epsilon, 0) &= \frac{2\epsilon(2\epsilon - 1)}{m^4} \text{ (circle with horizontal line) } , \\ F_6(\epsilon, 0) &= -\frac{2(\epsilon + 1)(2\epsilon - 1)}{m^4} \text{ (circle with horizontal line) } . \end{aligned} \quad (6.10)$$

In this way, we obtain the boundary values

$$I_5(\epsilon, 0) = 0, \quad I_6(\epsilon, 0) = -1 - 2\zeta_2\epsilon^2 + 2\zeta_3\epsilon^3 - 9\zeta_4\epsilon^4 + \mathcal{O}(\epsilon^5) . \quad (6.11)$$

- The integration constants of $I_{12,16,19,20,26,27,32,33}$ are fixed by demanding finiteness in the $t \rightarrow 4m^2$ limit and by demanding that the resulting boundary constants are real.
- The integrals I_{17} and I_{18} are regular in the $s \rightarrow 0$ limit. By imposing the regularity on their DEQ we can only fix the constant of one of them, say I_{18} . The boundary constants of I_{17} must be then computed in an independent way. We observe that the value of $I_{17}(\epsilon, 0)$ can be obtained in the limit $p_1^2 \rightarrow m^2$ of a similar vertex integral with off-shell momentum p_1^2 and $s \equiv (p_1 + p_2)^2 = p_2^2 = 0$,

$$I_{17}(\epsilon, 0) = \epsilon^4 m^2 \lim_{p_1^2 \rightarrow m^2} \text{ (triangle diagram with } p_1, p_2 \text{ and } s=0 \text{) } . \quad (6.12)$$

We discuss the computation of the auxiliary vertex integral in appendix A, where we show that the limit appearing in the r.h.s. of eq. (6.12) is indeed smooth and gives,

$$I_{17}(\epsilon, 0) = -\frac{27}{4}\zeta_4\epsilon^4 + \mathcal{O}(\epsilon^5) . \quad (6.13)$$

- The regularity of the four-point integrals $I_{21,22,25,28, \dots, 31}$ in either $s \rightarrow 0$ or $t \rightarrow 4m^2$ provides two boundary conditions, which can be complemented with additional relations obtained by imposing the regularity of the integrals at $s = -t = m^2/2$.
- The boundary constants of integral I_{24} are determined by demanding regularity in the limit $s \rightarrow -m^2$ and $t \rightarrow 4m^2$.
- The boundary constants of I_{34} are found by demanding finiteness in the limit $u \rightarrow \infty$.

All results have been numerically checked with the help of the computer codes `GiNaC` and `SecDec`, and the analytic expressions of the MIs are given in electronic form in the ancillary files attached to the `arXiv` version of this manuscript.

6.2 The second integral family

For the two-loop integral family defined in (3.6), we identify 42 MIs obeying an ϵ -linear system of DEQs:

$$\begin{aligned}
 F_1 &= \epsilon^2 \mathcal{T}_1, & F_2 &= \epsilon^2 \mathcal{T}_2, & F_3 &= \epsilon^2 \mathcal{T}_3, \\
 F_4 &= \epsilon^2 \mathcal{T}_4, & F_5 &= \epsilon^2 \mathcal{T}_5, & F_6 &= \epsilon^2 \mathcal{T}_6, \\
 F_7 &= \epsilon^2 \mathcal{T}_7, & F_8 &= \epsilon^2 \mathcal{T}_8, & F_9 &= \epsilon^2 \mathcal{T}_9, \\
 F_{10} &= \epsilon^2 \mathcal{T}_{10}, & F_{11} &= \epsilon^2 \mathcal{T}_{11}, & F_{12} &= \epsilon^3 \mathcal{T}_{12}, \\
 F_{13} &= \epsilon^2 \mathcal{T}_{13}, & F_{14} &= \epsilon^2 \mathcal{T}_{14}, & F_{15} &= \epsilon^3 \mathcal{T}_{15}, \\
 F_{16} &= \epsilon^2 \mathcal{T}_{16}, & F_{17} &= \epsilon^2 \mathcal{T}_{17}, & F_{18} &= \epsilon^3 \mathcal{T}_{18}, \\
 F_{19} &= \epsilon^3 \mathcal{T}_{19}, & F_{20} &= \epsilon^2 \mathcal{T}_{20}, & F_{21} &= \epsilon^3 \mathcal{T}_{21}, \\
 F_{22} &= \epsilon^2 \mathcal{T}_{22}, & F_{23} &= \epsilon^3 \mathcal{T}_{23}, & F_{24} &= \epsilon^2 \mathcal{T}_{24}, \\
 F_{25} &= \epsilon^3 \mathcal{T}_{25}, & F_{26} &= (1 - 2\epsilon)\epsilon^3 \mathcal{T}_{26}, & F_{27} &= \epsilon^3 \mathcal{T}_{27}, \\
 F_{28} &= \epsilon^2 \mathcal{T}_{28}, & F_{29} &= \epsilon^3 \mathcal{T}_{29}, & F_{30} &= \epsilon^2 \mathcal{T}_{30}, \\
 F_{31} &= (1 - 2\epsilon)\epsilon^3 \mathcal{T}_{31}, & F_{32} &= \epsilon^3 \mathcal{T}_{32}, & F_{33} &= \epsilon^4 \mathcal{T}_{33}, \\
 F_{34} &= \epsilon^3 \mathcal{T}_{34}, & F_{35} &= \epsilon^3 \mathcal{T}_{35}, & F_{36} &= \epsilon^4 \mathcal{T}_{36}, \\
 F_{37} &= \epsilon^4 \mathcal{T}_{37}, & F_{38} &= \epsilon^3 \mathcal{T}_{38}, & F_{39} &= \epsilon^4 \mathcal{T}_{39}, \\
 F_{40} &= \epsilon^4 \mathcal{T}_{40}, & F_{41} &= \epsilon^4 \mathcal{T}_{41}, & F_{42} &= \epsilon^4 (\mathcal{T}_{26} + \mathcal{T}_{42}), \quad (6.14)
 \end{aligned}$$

where the \mathcal{T}_i are depicted in figure 5. Through the Magnus exponential, we identify the corresponding canonical basis:

$$\begin{aligned}
 I_1 &= F_1, & I_2 &= -t F_2, \\
 I_3 &= \lambda_t F_3, & I_4 &= -t F_4, \\
 I_5 &= \frac{1}{2}(\lambda_t - t) F_4 - \lambda_t F_5, & I_6 &= -s F_6, \\
 I_7 &= 2m^2 F_6 + (m^2 - s) F_7, & I_8 &= m^2 F_8, \\
 I_9 &= m^2 F_9, & I_{10} &= -s F_{10}, \\
 I_{11} &= -t \lambda_t F_{11}, & I_{12} &= -t F_{12}, \\
 I_{13} &= -t m^2 F_{13}, & I_{14} &= -m^2(\lambda_t - t) \left(\frac{3}{2} F_{12} + F_{13} \right) \\
 & & & \quad - m^2 \lambda_t F_{14}, \\
 I_{15} &= \lambda_t F_{15}, & I_{16} &= m^2 \lambda_t F_{16}, \\
 I_{17} &= m^2(t - \lambda_t) \left(\frac{3}{2} F_{15} + F_{16} \right) - m^2 t F_{17}, & I_{18} &= \lambda_t F_{18}, \\
 I_{19} &= (m^2 - s) F_{19}, & I_{20} &= m^2(m^2 - s) F_{20}, \\
 I_{21} &= (m^2 - s) F_{21}, & I_{22} &= -\frac{3}{2} s F_9 + (s^2 - m^4) F_{22}, \\
 I_{23} &= \lambda_t F_{23}, & I_{24} &= \frac{1}{4} (4m^2 - t + \lambda_t) (F_4 + 2F_5) \\
 & & & \quad + m^2(4m^2 - t) F_{24},
 \end{aligned}$$

$$\begin{aligned}
 I_{25} &= \lambda_t F_{25}, & I_{26} &= -t F_{26}, \\
 I_{27} &= s t F_{27}, & I_{28} &= -m^4 t F_{27} - m^2(m^2 - s) t F_{28}, \\
 I_{29} &= -s \lambda_t F_{29}, & I_{30} &= m^4 \lambda_t F_{29} + m^2(m^2 - s) \lambda_t F_{30}, \\
 I_{31} &= -(m^2 - s) F_{31} \\
 &\quad - (m^2 - s)(4m^2 - t + \lambda_t) F_{31}, & I_{32} &= (m^2 - s) \lambda_t F_{32}, \\
 I_{33} &= (m^2 - s - t) F_{33}, & I_{34} &= (m^2 - s) \lambda_t F_{34}, \\
 I_{35} &= 2 \frac{m^4(m^2 - s)}{2m^2 - t - \lambda_t} F_{34} + m^2(m^2 - s) F_{35}, & I_{36} &= \lambda_t F_{36}, \\
 I_{37} &= -t(4m^2 - t) F_{37}, & I_{38} &= -(m^2 - s) t F_{38}, \\
 I_{39} &= -(m^2 - s) t F_{39}, & I_{40} &= -(m^2 - s) t \lambda_t F_{40}, \\
 I_{41} &= t \lambda_t (F_{40} - F_{41}), \\
 I_{42} &= (m^2 - t + \lambda_t) \\
 &\quad \times \left(\frac{2}{3} F_3 + \frac{1}{4} F_4 + \frac{1}{2} F_5 - \frac{1}{2} t F_{11} + \frac{5}{2} F_{12} + \frac{5}{3} m^2 F_{13} + \frac{5}{3} m^2 F_{14} \right. \\
 &\quad \quad \quad \left. + 2 F_{36} - \frac{1}{2} (m^2 + s) F_{40} + t F_{41} \right) \\
 &\quad + m^2 \left(\frac{1}{3} F_3 - \frac{1}{2} t F_{11} + \frac{1}{2} F_{12} + \frac{1}{3} m^2 F_{13} + \frac{1}{3} m^2 F_{14} + \frac{1}{2} F_{18} - \frac{1}{2} F_{40} \right) \\
 &\quad - t(m^2 - s) F_{11} - 2 \frac{m^4}{2m^2 - t - \lambda_t} F_{15} + t F_{26} + \frac{m^2(m^2 - s)(t + \lambda_t)}{2m^2 - t - \lambda_t} \left(\frac{2}{3} F_{29} - F_{34} \right) \\
 &\quad - \frac{2 m^2 s (t - \lambda_t)}{3(2m^2 - t - \lambda_t)} F_{29} + 2t F_{33} + \frac{4}{3} t m^4 \frac{m^2 - s}{\lambda_t + t} F_{30} - t F_{42}, \tag{6.15}
 \end{aligned}$$

which satisfies a system of DEQs of the form in eq. (4.4), whose corresponding 42×42 matrices are collected in appendix B.2. We observe that $I_{1,2,6,7,8,10,15,16,17,27,28}$ correspond, respectively, to $I_{1,3,5,6,4,2,13,14,15,23,24}$ of integral family (3.5) previously discussed. The boundary constants of the remaining integrals can be fixed in the following way:

- The integration constants of $I_{3,4,5,11,\dots,14,18,23,24,26,29,\dots,35}$ by demanding regularity in the limit $t \rightarrow 0$.
- The boundary values of I_9 can be obtained by direct integration and it is given by

$$\begin{aligned}
 I_9(\epsilon) &= -\frac{\zeta_2}{2} \epsilon^2 + \frac{1}{4} (12\zeta_2 \log(2) - 7\zeta_3) \epsilon^3 \\
 &\quad + \left(-12\text{Li}_4\left(\frac{1}{2}\right) + \frac{31}{40} \zeta_4 - \frac{\log^4(2)}{2} - 6\zeta_2 \log^2(2) \right) \epsilon^4 + \mathcal{O}(\epsilon^5). \tag{6.16}
 \end{aligned}$$

- The boundary constants of $I_{19,21}$ can be fixed by demanding regularity when $s \rightarrow 0$.
- The boundary constants of $I_{20,22,25}$ are determined by demanding regularity, respectively, when $s \rightarrow -\frac{1}{2}(2m^2 - t - \lambda_t)$, $s \rightarrow -m^2$, and $t \rightarrow 4m^2$.
- Finally, the boundary constants of $I_{36\dots 42}$ can be all determined by demanding regularity in the simultaneous limits $t \rightarrow \frac{9}{2}m^2$ and $s \rightarrow -2m^2$.

All results have been numerically checked with the help of the computer codes `GiNaC` and `SecDec`, and the analytic expressions of the MIs are given in electronic form in the ancillary files attached to the `arXiv` version of this manuscript.

7 Towards the non-planar integrals

The complete computation of the NNLO virtual QED corrections to μe scattering requires the evaluation of one last missing four-point topology, which corresponds to the non-planar diagram T_6 of figure 1. In view of future studies dedicated to this last class of integrals, we hereby show how the previously adopted strategy, based on differential equations, Magnus exponential and regularity conditions, can be efficiently applied to compute the MIs of a simpler vertex integral belonging to same family.

7.1 Master integrals for the non-planar vertex

We consider the non-planar vertex depicted in figure 6, whose integral family is defined as

$$\int \widetilde{d^d k_1} \widetilde{d^d k_2} \frac{D_4^{n_4}}{D_1^{n_1} D_2^{n_2} D_3^{n_3} D_5^{n_5} D_6^{n_6} D_7^{n_7}}, \quad n_i \geq 0, \quad (7.1)$$

where the loop propagators are chosen to be

$$\begin{aligned} D_1 &= k_1^2 - m^2, & D_2 &= k_2^2 - m^2, \\ D_3 &= (k_1 + p_1 + p_2)^2, & D_4 &= (k_2 + p_1 + p_2)^2, \\ D_5 &= (k_1 - k_2 + p_3)^2, & D_6 &= (k_2 + p_4)^2, & D_7 &= (k_1 - k_2)^2. \end{aligned} \quad (7.2)$$

The MIs belonging to this integral family, which will be part of the full set of MIs needed for the computation of T_6 , have been already considered in the literature [25–29]. In all previous computations, the determination of the boundary constants resorted either to the fitting of numerical values to transcendental constants [25–27] or to Mellin-Barnes techniques [29]. With the present calculation, we show that they can be fixed equivalently by imposing the regularity of the solution at specific kinematic pseudo-thresholds and by matching a particular linear combination of integrals to their massless counterpart.

In order to determine the MIs belonging to the integral family (7.1), we derive their DEQ in the dimensionless variable x . We identify a set of 14 MIs which fulfills an ϵ -linear system of DEQs,

$$\begin{aligned} F_1 &= \epsilon^2 \mathcal{T}_1, & F_2 &= \epsilon^2 \mathcal{T}_2, & F_3 &= \epsilon^2 \mathcal{T}_3, \\ F_4 &= \epsilon^2 \mathcal{T}_4, & F_5 &= \epsilon^2 \mathcal{T}_5, & F_6 &= \epsilon^3 \mathcal{T}_6, \\ F_7 &= \epsilon^2 \mathcal{T}_7, & F_8 &= \epsilon^3 \mathcal{T}_8, & F_9 &= \epsilon^2 \mathcal{T}_9, \\ F_{10} &= \epsilon^2 \mathcal{T}_{10}, & F_{11} &= \epsilon^2 (2\epsilon - 1) \mathcal{T}_{11}, & F_{12} &= \epsilon^4 \mathcal{T}_{12}, \\ F_{13} &= \epsilon^3 \mathcal{T}_{13}, & F_{14} &= \epsilon^4 \mathcal{T}_{14}, \end{aligned} \quad (7.3)$$

where the \mathcal{T}_i are depicted in figure 7.

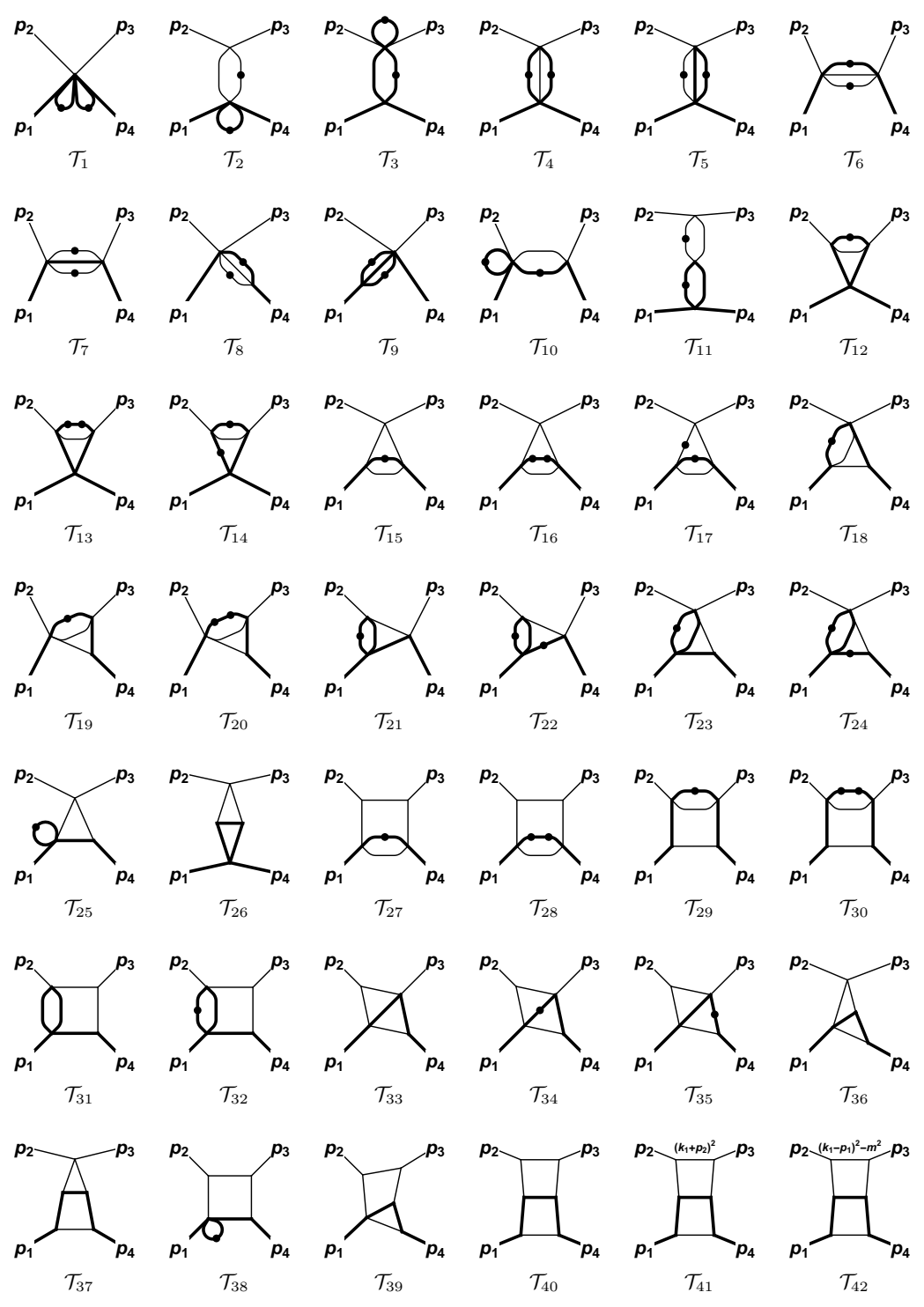


Figure 5. Two-loop MIs $\mathcal{T}_{1,\dots,42}$ for the second integral family.

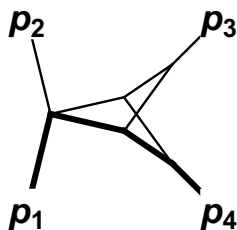


Figure 6. Non-planar two-loop three-point topology.

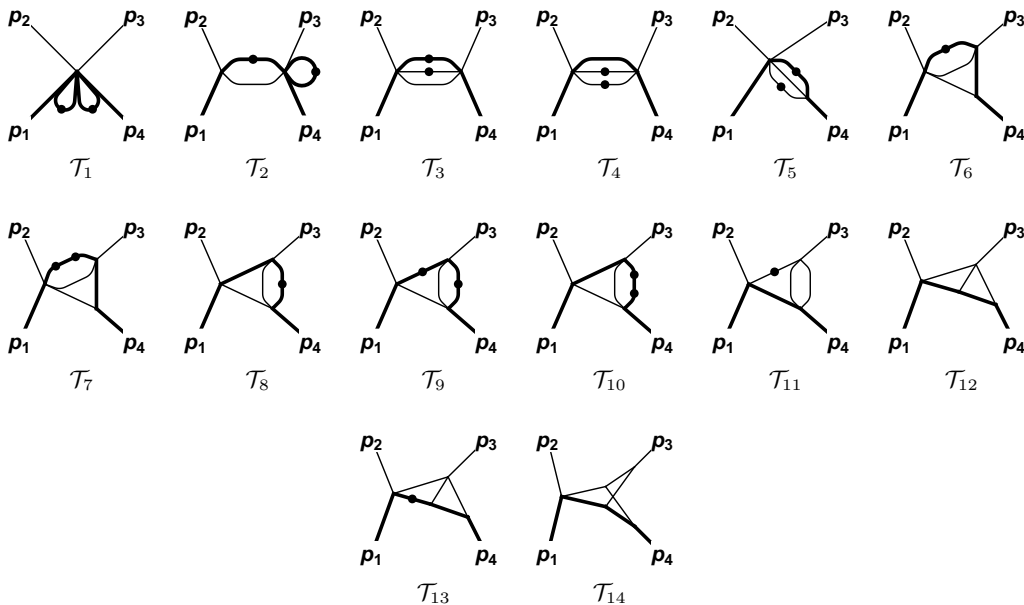


Figure 7. Two-loop MIs $\mathcal{T}_{1,\dots,14}$ for the non-planar vertex.

By making use of the Magnus exponential, we can transform these MIs into the canonical basis

$$\begin{aligned}
 I_1 &= F_1, & I_2 &= -s F_2, \\
 I_3 &= -s F_3, & I_4 &= 2m^2 F_3 + (m^2 - s) F_4, \\
 I_5 &= m^2 F_5, & I_6 &= (m^2 - s) F_6, \\
 I_7 &= m^2(m^2 - s) F_7, & I_8 &= (m^2 - s) F_8, \\
 I_9 &= m^2 (3 F_8 + (2m^2 - s) F_9 + 2m^2 F_{10}), & I_{10} &= m^2(m^2 - s) F_{10}, \\
 I_{11} &= \frac{1}{(s + m^2)} (-2m^4 F_5 + (s - m^2)s F_{11}), & I_{12} &= (m^2 - s) F_{12}, \\
 I_{13} &= m^2(m^2 - s) F_{13}, & I_{14} &= (m^2 - s)^2 F_{14},
 \end{aligned} \tag{7.4}$$

The computation of the auxiliary vertex integrals, which is discussed in appendix A, leads to

$$\begin{aligned}
 I_8(\epsilon, 0) &= \left(\frac{5\zeta_3}{4} - 3\zeta_2 \log(2) \right) \epsilon^3 + \left(8\text{Li}_4 \left(\frac{1}{2} \right) - \frac{33}{8}\zeta_4 + \frac{\log^4(2)}{3} - 2\zeta_2 \log^2(2) \right) \epsilon^4, \\
 I_{10}(\epsilon, 0) &= \frac{\pi^2}{12} \epsilon^2 + \left(\frac{\zeta_3}{4} + 3\zeta_2 \log(2) \right) \epsilon^3 \\
 &\quad + \left(-8\text{Li}_4 \left(\frac{1}{2} \right) + \frac{65}{4}\zeta_4 - \frac{\log^4(2)}{3} + 2\zeta_2 \log^2(2) \right) \epsilon^4 + \mathcal{O}(\epsilon^5). \tag{7.8}
 \end{aligned}$$

- The boundary constant of I_{11} is determined by imposing regularity when $s \rightarrow 0$.
- I_{12} corresponds to I_{17} of the integral family (3.5) and the boundary constant of I_{13} can be fixed by demanding regularity when $s \rightarrow 0$.
- The boundary condition for I_{14} is determined from the $m \rightarrow 0$, or equivalently $s \rightarrow \infty$ behaviour of the solutions, where all the internal lines of the diagrams become *massless*. In this regime, we search for a combination of integrals behaving as,

$$\lim_{z \rightarrow 0} \sum_i c_i I_i = z^{a\epsilon} F(\epsilon), \quad a \in \mathbb{Z}, \tag{7.9}$$

where $F(\epsilon)$ is finite as $z \rightarrow 0$.

Following the ideas outlined in [68], we begin by performing a change of variables $z = 1/x = (-m^2/s)$, yielding a total differential equation of the form,

$$d\mathbf{I} = \epsilon \left(\mathbb{M}_1 d\log(z) + \mathbb{M}_2 d\log(1+z) + \mathbb{M}_3 d\log(1+2z) \right) \mathbf{I}, \tag{7.10}$$

where \mathbb{M}_i are the constant matrices

$$\begin{aligned}
 \mathbb{M}_1 &= \begin{pmatrix} 0 & 0 & 0 & 0 & 0 & 0 & 0 & 0 & 0 & 0 & 0 & 0 & 0 & 0 & 0 \\ 1 & 1 & 0 & 0 & 0 & 0 & 0 & 0 & 0 & 0 & 0 & 0 & 0 & 0 & 0 \\ 0 & 0 & 1 & 1 & 0 & 0 & 0 & 0 & 0 & 0 & 0 & 0 & 0 & 0 & 0 \\ 0 & 0 & 0 & 2 & 0 & 0 & 0 & 0 & 0 & 0 & 0 & 0 & 0 & 0 & 0 \\ 0 & 0 & 0 & 0 & 0 & 0 & 0 & 0 & 0 & 0 & 0 & 0 & 0 & 0 & 0 \\ \frac{1}{2} & 0 & -\frac{1}{2} & 0 & 1 & 2 & 0 & 0 & 0 & 0 & 0 & 0 & 0 & 0 & 0 \\ -\frac{1}{2} & 0 & \frac{1}{2} & -\frac{1}{2} & 0 & 0 & 0 & 0 & 0 & 0 & 0 & 0 & 0 & 0 & 0 \\ \frac{1}{2} & 0 & 0 & 0 & 2 & 0 & 0 & 2 & 2 & 0 & 0 & 0 & 0 & 0 & 0 \\ 0 & 0 & 0 & 0 & 0 & 0 & 0 & 0 & 0 & 0 & 0 & 0 & 0 & 0 & 0 \\ 0 & \frac{1}{2} & 0 & 0 & 0 & 0 & 0 & -1 & 0 & 0 & 0 & 0 & 0 & 0 & 0 \\ 0 & 0 & 0 & 0 & 0 & 0 & 0 & 0 & 0 & 0 & 2 & 0 & 0 & 0 & 0 \\ -\frac{1}{4} & 0 & 0 & -\frac{1}{4} & -1 & 0 & 0 & 0 & 0 & 0 & -\frac{1}{2} & 1 & 2 & 0 & 0 \\ \frac{1}{2} & \frac{1}{2} & -\frac{1}{2} & -\frac{1}{2} & 0 & 0 & 0 & 0 & 0 & 0 & 0 & 0 & 0 & 0 & 0 \\ -1 & -1 & -\frac{4}{3} & -\frac{2}{3} & -4 & -3 & -4 & 0 & -2 & 2 & -1 & -2 & -2 & 2 & 0 \end{pmatrix}, \quad \mathbb{M}_2 = \begin{pmatrix} 0 & 0 & 0 & 0 & 0 & 0 & 0 & 0 & 0 & 0 & 0 & 0 & 0 & 0 & 0 \\ -1 & -2 & 0 & 0 & 0 & 0 & 0 & 0 & 0 & 0 & 0 & 0 & 0 & 0 & 0 \\ 0 & 0 & -2 & -1 & 0 & 0 & 0 & 0 & 0 & 0 & 0 & 0 & 0 & 0 & 0 \\ 0 & 0 & -4 & -2 & 0 & 0 & 0 & 0 & 0 & 0 & 0 & 0 & 0 & 0 & 0 \\ 0 & 0 & 0 & 0 & 0 & 0 & 0 & 0 & 0 & 0 & 0 & 0 & 0 & 0 & 0 \\ 0 & 0 & 0 & 0 & 0 & 2 & 0 & 0 & 0 & 0 & 0 & 0 & 0 & 0 & 0 \\ 0 & 0 & 0 & 0 & 0 & -3 & -2 & 0 & 0 & 0 & 0 & 0 & 0 & 0 & 0 \\ 0 & 0 & 0 & 0 & 0 & 0 & 2 & 0 & 0 & 0 & 0 & 0 & 0 & 0 & 0 \\ -\frac{3}{2} & -1 & 0 & 0 & -6 & 0 & 0 & -6 & -4 & -2 & 0 & 0 & 0 & 0 & 0 \\ 0 & 0 & 0 & 0 & 0 & 0 & -3 & 0 & -2 & 0 & 0 & 0 & 0 & 0 & 0 \\ 0 & 0 & 0 & 0 & -4 & 0 & 0 & 0 & 0 & 0 & -4 & 0 & 0 & 0 & 0 \\ 0 & 0 & 0 & 0 & 0 & 0 & 0 & 0 & 0 & 0 & 0 & 0 & 2 & 0 & 0 \\ 0 & 0 & 0 & 0 & 0 & 0 & 0 & 0 & 0 & 0 & 0 & 0 & -6 & -4 & 0 \\ 1 & 1 & \frac{4}{3} & \frac{2}{3} & 4 & 3 & 4 & 0 & 2 & -2 & 1 & 2 & 2 & -2 & 0 \end{pmatrix}, \\
\mathbb{M}_3 &= \begin{pmatrix} 0 & 0 & 0 & 0 & 0 & 0 & 0 & 0 & 0 & 0 & 0 & 0 & 0 & 0 & 0 \\ 0 & 0 & 0 & 0 & 0 & 0 & 0 & 0 & 0 & 0 & 0 & 0 & 0 & 0 & 0 \\ 0 & 0 & 0 & 0 & 0 & 0 & 0 & 0 & 0 & 0 & 0 & 0 & 0 & 0 & 0 \\ 0 & 0 & 0 & 0 & 0 & 0 & 0 & 0 & 0 & 0 & 0 & 0 & 0 & 0 & 0 \\ 0 & 0 & 0 & 0 & 0 & 0 & 0 & 0 & 0 & 0 & 0 & 0 & 0 & 0 & 0 \\ 0 & 0 & 0 & 0 & 0 & 0 & 0 & 0 & 0 & 0 & 0 & 0 & 0 & 0 & 0 \\ 0 & 0 & 0 & 0 & 0 & 0 & 0 & 0 & 0 & 0 & 0 & 0 & 0 & 0 & 0 \\ 0 & 0 & 0 & 0 & 0 & 0 & -3 & -1 & -2 & 0 & 0 & 0 & 0 & 0 & 0 \\ 0 & 0 & 0 & 0 & 0 & 0 & 3 & 1 & 2 & 0 & 0 & 0 & 0 & 0 & 0 \\ 0 & 0 & 0 & 0 & 0 & 0 & 3 & 1 & 2 & 0 & 0 & 0 & 0 & 0 & 0 \\ 0 & 0 & 0 & 0 & 0 & 0 & 0 & 0 & 0 & 0 & 0 & 0 & 0 & 0 & 0 \\ 0 & 0 & 0 & 0 & 0 & 0 & 0 & 0 & 0 & 0 & 0 & 0 & 0 & 0 & 0 \\ 0 & 0 & 0 & 0 & 0 & 0 & 0 & 0 & 0 & 0 & 0 & 0 & 0 & 0 & 0 \\ 0 & 0 & 0 & 0 & 0 & 0 & 0 & 0 & 0 & 0 & 0 & 0 & 0 & 0 & 0 \end{pmatrix}. \tag{7.11}
 \end{aligned}$$

\mathbf{I} must be evaluated in the limit $m \rightarrow 0$ (or alternatively $s \rightarrow \infty$). To this aim, we need to pull out the prefactor $m^{4\epsilon}$ coming from the integration measure defined in eq. (3.2), and to consider the definition of the canonical integrals \mathbf{I} in terms of the linear- ϵ basis \mathbf{F} given in eq. (7.4),

$$\mathbf{H}_{11,0} = (-s)^{2\epsilon} \left(2sF_3 + 3sF_6 - sF_{11} + 2sF_{12} + s^2F_{14} \right) \Big|_{m=0}. \quad (7.19)$$

In the latter equation, we took into account the vanishing of the massless tadpole in dimensional regularisation and the symmetries arising from the massless limit of the \mathbf{F} integrals. After applying the IBPs to the massless integrals, the contributions due to all subtopologies cancel and the contribution of the *massless non-planar vertex* $F_{14}|_{m=0}$ [23] is the only one left,

$$\mathbf{H}_{11,0} = (-s)^{2+2\epsilon} F_{14}|_{m=0}, \quad (7.20)$$

where

$$F_{14}|_{m=0} = (-s)^{-2-2\epsilon} \mathcal{F}(\epsilon) \quad (7.21)$$

with

$$\mathcal{F}(\epsilon) \equiv 1 - 7\zeta_2\epsilon^2 - 27\zeta_3\epsilon^3 - \frac{57}{2}\zeta_4\epsilon^4 + \mathcal{O}(\epsilon^5). \quad (7.22)$$

Therefore,

$$\mathbf{H}_{11,0} = \mathcal{F}(\epsilon). \quad (7.23)$$

Finally the boundary constant of integral I_{14} can be determined by demanding the equality of eq. (7.18) and eq. (7.23).

All results have been numerically checked with the help of the computer codes `GiNaC` and `SecDec`, and the analytic expressions of the MIs are given in electronic form in the ancillary files attached to the `arXiv` version of this manuscript.

8 Conclusions

The scattering of high-energy muons on atomic electrons has been recently proposed as an ideal framework to determine the leading hadronic contribution to the anomalous magnetic moment of the muon. The ambitious experimental goal of measuring the differential cross section of the $\mu e \rightarrow \mu e$ process with an accuracy of 10ppm requires, on the theoretical side, the knowledge of the QED corrections at NNLO. In this work, after calculating the QED corrections at NLO, which were found to be in agreement with the latest results in the literature, we investigated the feasibility of the evaluation of the corrections at NNLO. In particular, we began by considering the two-loop planar box-diagrams contributing to this process. We employed the method of differential equations and of the Magnus exponential series to identify a canonical set of master integrals. Boundary conditions

were derived from the regularity requirements at pseudothresholds, or from the knowledge of the integrals at special kinematic points, evaluated by means of auxiliary, simpler systems of differential equations.

The considered master integrals were expressed as a Taylor series around four space-time dimensions, whose coefficients are written as a combination of generalised polylogarithms. We worked in the massless electron approximation, while keeping full dependence on the muon mass. Besides μe scattering, our results are relevant also for crossing-related processes such as muon-pair production at e^+e^- -colliders, as well as for the QCD corrections to top -pair production at hadron colliders.

The evaluation of the missing contributions due to non-planar box graphs will be the subject of a dedicated, future work — we are confident that the techniques employed here can be systematically applied for that case as well.

Acknowledgments

We thank Roberto Bonciani, Matteo Fael, Andrea Ferroglia and Stefano Laporta for useful discussions. We are happy to acknowledge the stimulating discussions which took place during the workshops *Muon-electron scattering: theory kick-off meeting* (4–6 September 2017, Padova, Italy) and *Flavor Changing and Conserving Processes 2017* (7–9 September 2017, Anacapri, Capri Island, Italy). We wish to thank also Federico Gasparotto, for checks on the one-loop MIs.

This research was supported in part by Perimeter Institute for Theoretical Physics. Research at Perimeter Institute is supported by the Government of Canada through the Department of Innovation, Science and Economic Development and by the Province of Ontario through the Ministry of Research, Innovation and Science. The work of U. S. was performed in part at the Aspen Center for Physics, which is supported by the National Science Foundation grant PHY-1607611. U. S. is supported by the DOE contract DE-AC02-06CH11357. A. P. wishes to thank the Institute for Particle Physics (IFIC) of Valencia for hospitality during the final stages of this project. M. P. acknowledges partial support by FP10 ITN Elusives (H2020-MSCA-ITN-2015-674896) and Invisibles-Plus (H2020-MSCA-RISE-2015-690575).

A Auxiliary integrals

In this appendix we briefly discuss the solution of the system of differential equations for the vertex integrals which has been used in eqs. (6.12) and (7.7) as an input for the determination of the boundary constants of some of the MIs considered in this paper.

Auxiliary vertex integral for eq. (6.12). We consider the integral family

$$\int \widetilde{d^d k_1} \widetilde{d^d k_2} \frac{D_6^{n_6} D_7^{n_7}}{D_1^{n_1} D_2^{n_2} D_3^{n_3} D_4^{n_4} D_5^{n_5}}, \quad n_i \geq 0, \quad (\text{A.1})$$

identified by the set of denominators

$$\begin{aligned} D_1 &= k_1^2 - m^2, & D_2 &= k_2^2 - m^2, & D_3 &= (k_1 + p_1)^2, & D_4 &= (k_2 + p_1 + p_2)^2, \\ D_5 &= (k_1 - k_2)^2, & D_6 &= (k_2 + p_1)^2, & D_7 &= (k_1 + p_1 + p_2)^2, \end{aligned} \quad (\text{A.2})$$

and by external momenta p_1 , p_2 and p_3 satisfying

$$p_2^2 = 0, \quad p_3^2 = (p_1 + p_2)^2 = 0. \quad (\text{A.3})$$

All integrals belonging to this family can be reduced to a set of 8 MIs, whose dependence on p_1^2 is parametrized in terms of the dimensionless variable

$$x = -\frac{p_1^2}{m^2}. \quad (\text{A.4})$$

The basis of integrals

$$\begin{aligned} I_1 &= \epsilon^2 \langle \text{figure 1} \rangle, & I_2 &= -\epsilon^2 p_1^2 \langle \text{figure 2} \rangle, \\ I_3 &= -\epsilon^2 p_1^2 \langle \text{figure 3} \rangle, & I_4 &= \epsilon^2 2m^2 \langle \text{figure 4} \rangle + \epsilon^2 (m^2 - p_1^2) \langle \text{figure 5} \rangle, \\ I_5 &= \epsilon(1 - \epsilon)m^2 \langle \text{figure 6} \rangle, & I_6 &= -\epsilon^3 p_1^2 \langle \text{figure 7} \rangle, \\ I_7 &= -\epsilon^4 p_1^2 \langle \text{figure 8} \rangle, & I_8 &= \epsilon^3 p_1^2 (p_1^2 - m^2) \langle \text{figure 9} \rangle. \end{aligned} \quad (\text{A.5})$$

fulfills a canonical system of differential equations,

$$d\mathbf{I} = \epsilon d\mathbb{A} \mathbf{I}, \quad (\text{A.6})$$

where

$$d\mathbb{A} = \mathbb{M}_1 d\log x + \mathbb{M}_2 d\log(1 + x), \quad (\text{A.7})$$

with

$$\mathbb{M}_1 = \begin{pmatrix} 0 & 0 & 0 & 0 & 0 & 0 & 0 & 0 \\ 0 & 1 & 0 & 0 & 0 & 0 & 0 & 0 \\ 0 & 0 & 1 & 0 & 0 & 0 & 0 & 0 \\ 0 & 0 & 0 & 4 & 0 & 0 & 0 & 0 \\ 0 & 0 & 0 & 0 & 0 & 0 & 0 & 0 \\ 0 & 0 & 0 & 0 & 0 & 1 & 0 & 0 \\ 0 & -\frac{1}{4} & -\frac{1}{2} & 0 & 0 & \frac{1}{4} & \frac{1}{2} & \frac{3}{4} \\ 0 & -\frac{1}{2} & -1 & 0 & 0 & \frac{1}{2} & -1 & \frac{5}{2} \end{pmatrix}, \quad \mathbb{M}_2 = \begin{pmatrix} 0 & 0 & 0 & 0 & 0 & 0 & 0 & 0 \\ -1 & -2 & 0 & 0 & 0 & 0 & 0 & 0 \\ 0 & 0 & -2 & -1 & 0 & 0 & 0 & 0 \\ 0 & 0 & -4 & -2 & 0 & 0 & 0 & 0 \\ 0 & 0 & 0 & 0 & 0 & 0 & 0 & 0 \\ 0 & 0 & 0 & 0 & -\frac{1}{2} & -3 & 0 & 0 \\ 0 & 0 & 0 & 0 & 0 & 0 & 0 & 0 \\ 1 & 2 & 0 & 0 & -\frac{1}{2} & -3 & 0 & -4 \end{pmatrix}. \quad (\text{A.8})$$

In the Euclidean region $x > 0$ the general solution of the system of differential equations can be expressed in terms of harmonic polylogarithms (HPLs) [46], and the boundary constants of all master integrals, with the only exception of $I_1 = 1$ and

$$I_5(\epsilon) = 1 + 2\zeta_2\epsilon^2 - 2\zeta_3\epsilon^3 + 9\zeta_4\epsilon^4 + \mathcal{O}(\epsilon^5), \quad (\text{A.9})$$

can be fixed by demanding their regularity at $x \rightarrow 0$. In particular, for the $I_7(\epsilon, x)$ we obtain

$$I_7(\epsilon, x) = (-2\zeta_2 H(0, -1; x) - H(0, -1, -1, -1; x) + H(0, -1, 0, -1; x))\epsilon^4 + \mathcal{O}(\epsilon^5). \quad (\text{A.10})$$

This expression, when it is analytically continued to the region $x < 0$, has a smooth limit for $x \rightarrow -1$ ($p_1^2 = m^2$),

$$I_7(\epsilon, -1) = \frac{27}{4}\zeta_4\epsilon^4 + \mathcal{O}(\epsilon^5), \quad (\text{A.11})$$

which has been used in eq. (6.13).

Auxiliary vertex integral for eq. (7.7). We consider the integral family

$$\int \widetilde{d^d k_1} \widetilde{d^d k_2} \frac{D_5^{n_5} D_6^{n_6} D_7^{n_7}}{D_1^{n_1} D_2^{n_2} D_3^{n_3} D_4^{n_4}}, \quad n_i \geq 0, \quad (\text{A.12})$$

identified by the set of denominators

$$\begin{aligned} D_1 &= k_1^2, & D_2 &= k_2^2 - m^2, \\ D_3 &= (k_1 + p_1)^2 - m^2, & D_4 &= (k_1 + k_2 + p_1 + p_2)^2, \\ D_5 &= (k_1 + p_2)^2, & D_6 &= (k_2 + p_1)^2, & D_7 &= (k_2 + p_1 + p_2)^2, \end{aligned} \quad (\text{A.13})$$

and by external momenta p_1, p_2 and p_3 satisfying

$$p_1^2 = p_2^2 = 0, \quad (p_1 + p_2)^2 = p_3^2. \quad (\text{A.14})$$

All integrals belonging to this family can be reduced to a set of 5 MIs, whose dependence on p_3^2 is parametrized in terms of the dimensionless variable

$$x = -\frac{p_3^2}{m^2}. \quad (\text{A.15})$$

The basis of integrals

$$\begin{aligned} I_1 &= \epsilon^2 \text{ (figure-eight diagram) }, & I_2 &= -\epsilon^2 p_3^2 \text{ (fish diagram) }, \\ I_3 &= \epsilon^2 2m^2 \text{ (fish diagram) } + \epsilon^2 (m^2 - p_3^2) \text{ (fish diagram) }, \\ I_4 &= -\epsilon^3 p_3^2 \text{ (triangle diagram) }^{s=0}, & I_5 &= -\epsilon^4 p_3^2 m^2 \text{ (triangle diagram) }, \end{aligned} \quad (\text{A.16})$$

fulfils a canonical system of differential equations,

$$d\mathbf{I} = \epsilon d\mathbb{A} \mathbf{I}, \tag{A.17}$$

where

$$d\mathbb{A} = \mathbb{M}_1 d\log x + \mathbb{M}_2 d\log(1+x) + \mathbb{M}_3 d\log(1-x), \tag{A.18}$$

with

$$\mathbb{M}_1 = \begin{pmatrix} 0 & 0 & 0 & 0 & 0 \\ 0 & 1 & 0 & 0 & 0 \\ 0 & 4 & 0 & 0 & 0 \\ 0 & 0 & 0 & 1 & 0 \\ 0 & \frac{1}{2} & 0 & -2 & -2 \end{pmatrix}, \quad \mathbb{M}_2 = \begin{pmatrix} 0 & 0 & 0 & 0 & 0 \\ 0 & -2 & -1 & 0 & 0 \\ 0 & -4 & -2 & 0 & 0 \\ 0 & 0 & 0 & 0 & 0 \\ 0 & 0 & 0 & 0 & 0 \end{pmatrix}, \quad \mathbb{M}_3 = \begin{pmatrix} 0 & 0 & 0 & 0 & 0 \\ 0 & 0 & 0 & 0 & 0 \\ 0 & 0 & 0 & 0 & 0 \\ -\frac{1}{2} & 1 & -\frac{1}{2} & -2 & -2 \\ \frac{1}{2} & -1 & \frac{1}{2} & 2 & 2 \end{pmatrix}. \tag{A.19}$$

In the Euclidean region $x > 0$ the general solution of the system of differential equations can be expressed in terms of HPLs. The boundary constants $I_{4,5}$, which are the only MIs appearing for the first time in this computation, can be fixed by demanding their regularity at $x \rightarrow 0$. In this way, we obtain

$$I_i(\epsilon, x) = \sum_{k=2}^4 I_i^{(k)}(x, y) \epsilon^k + \mathcal{O}(\epsilon^5), \tag{A.20}$$

with

$$\begin{aligned} I_4^{(2)}(x) &= 0, \\ I_4^{(3)}(x) &= -\zeta_2 H(1; x) + 2H(1, 0, -1; x), \\ I_4^{(4)}(x) &= \zeta_3 H(1; x) - \zeta_2 H(0, 1; x) + 2H(0, 1, 0, -1; x) - 8H(1, 0, -1, -1; x), \end{aligned} \tag{A.21}$$

and

$$\begin{aligned} I_5^{(2)}(x) &= \frac{1}{2} H(0, -1; x), \\ I_5^{(3)}(x) &= \zeta_2 H(1; x) - 2H(0, -1, -1; x) - \frac{1}{2} H(0, 0, -1; x) - 2H(1, 0, -1; x), \\ I_5^{(4)}(x) &= -\zeta_3 H(1; x) + \zeta_2 H(0, -1; x) 8H(0, -1, -1, -1; x) - 3H(0, -1, 0, -1; x) \\ &\quad + 2H(0, 0, -1, -1; x) + \frac{3}{2} H(0, 0, 0, -1; x) + 8H(1, 0, -1, -1; x). \end{aligned} \tag{A.22}$$

The analytic continuation of these expressions to $x \rightarrow -1$ ($p_3^2 = m^2$) produces the smooth limits

$$\begin{aligned} I_4(\epsilon, -1) &= -\left(\frac{5\zeta_3}{4} - 3\zeta_2 \log(2)\right) \epsilon^3 - \left(8\text{Li}_4\left(\frac{1}{2}\right) - \frac{33}{8}\zeta_4 + \frac{\log^4(2)}{3} - 2\zeta_2 \log^2(2)\right) \epsilon^4, \\ I_5(\epsilon, -1) &= -\frac{\zeta_2}{2} \epsilon^2 - \left(\frac{\zeta_3}{4} + 3\zeta_2 \log(2)\right) \epsilon^3 \\ &\quad - \left(-8\text{Li}_4\left(\frac{1}{2}\right) + \frac{65}{4}\zeta_4 - \frac{\log^4(2)}{3} + 2\zeta_2 \log^2(2)\right) \epsilon^4 + \mathcal{O}(\epsilon^5), \end{aligned} \tag{A.23}$$

which have been used in eq. (7.8).

Open Access. This article is distributed under the terms of the Creative Commons Attribution License ([CC-BY 4.0](https://creativecommons.org/licenses/by/4.0/)), which permits any use, distribution and reproduction in any medium, provided the original author(s) and source are credited.

References

- [1] G. Backenstoss, B.D. Hyams, G. Knop, P.C. Marin and U. Stierlin, *Helicity of μ^- mesons from π -meson decay*, *Phys. Rev. Lett.* **6** (1961) 415 [[INSPIRE](#)].
- [2] G. Backenstoss, B.D. Hyams, G. Knop, P.C. Marin and U. Stierlin, *Scattering of 8 GeV μ mesons on electrons*, *Phys. Rev.* **129** (1963) 2759.
- [3] T. Kirk and S. Neddermeyer, *Scattering of high-energy positive and negative muons on electrons*, *Phys. Rev.* **171** (1968) 1412.
- [4] P.L. Jain and N.J. Wixon, *Scattering of high-energy positive and negative muons on electrons*, *Phys. Rev. Lett.* **23** (1969) 715 [[INSPIRE](#)].
- [5] R.F. Deery and S.H. Neddermeyer, *Cloud-chamber study of hard collisions of cosmic-ray muons with electrons*, *Phys. Rev.* **121** (1961) 1803.
- [6] I.B. McDiarmid and M.D. Wilson, *The production of high-energy knock-on electrons and bremsstrahlung by μ mesons*, *Can. J. Phys.* **40** (1962) 698.
- [7] N. Chaudhuri and M.S. Sinha, *Production of knock-on electrons by cosmic-ray muons underground (148 m w.e.)*, *Nuovo Cimento* **35** (1965) 13.
- [8] P.D. Kearney and W.E. Hazen, *Electromagnetic interactions of high-energy muons*, *Phys. Rev. B* **138** (1965) 173.
- [9] K.P. Schuler, *A muon polarimeter based on elastic muon electron scattering*, *AIP Conf. Proc.* **187** (1989) 1401 [[INSPIRE](#)].
- [10] SPIN MUON collaboration, D. Adams et al., *Measurement of the SMC muon beam polarization using the asymmetry in the elastic scattering off polarized electrons*, *Nucl. Instrum. Meth. A* **443** (2000) 1 [[INSPIRE](#)].
- [11] G. Abbiendi et al., *Measuring the leading hadronic contribution to the muon $g - 2$ via μe scattering*, *Eur. Phys. J. C* **77** (2017) 139 [[arXiv:1609.08987](#)] [[INSPIRE](#)].
- [12] C.M. Carloni Calame, M. Passera, L. Trentadue and G. Venanzoni, *A new approach to evaluate the leading hadronic corrections to the muon $g - 2$* , *Phys. Lett. B* **746** (2015) 325 [[arXiv:1504.02228](#)] [[INSPIRE](#)].
- [13] A.I. Nikishov, *Radiative corrections to the scattering of μ mesons on electrons*, *Sov. Phys. JETP* **12** (1961) 529.
- [14] K.E. Eriksson, *Radiative corrections to muon-electron scattering*, *Nuovo Cim.* **19** (1961) 1029.
- [15] K.E. Eriksson, B. Larsson and G.A. Rinander, *Radiative corrections to muon-electron scattering*, *Nuovo Cim.* **30** (1963) 1434.
- [16] P. Van Nieuwenhuizen, *Muon-electron scattering cross-section to order alpha-to-the-third*, *Nucl. Phys. B* **28** (1971) 429 [[INSPIRE](#)].
- [17] T.V. Kukhto, N.M. Shumeiko and S.I. Timoshin, *Radiative corrections in polarized electron muon elastic scattering*, *J. Phys. G* **13** (1987) 725 [[INSPIRE](#)].

- [18] D. Yu. Bardin and L. Kalinovskaya, *QED corrections for polarized elastic muon e scattering*, [hep-ph/9712310](#) [INSPIRE].
- [19] N. Kaiser, *Radiative corrections to lepton-lepton scattering revisited*, *J. Phys. G* **37** (2010) 115005 [INSPIRE].
- [20] E. Derman and W.J. Marciano, *Parity Violating Asymmetries in Polarized Electron Scattering*, *Annals Phys.* **121** (1979) 147 [INSPIRE].
- [21] G. D'Ambrosio, *Electron muon scattering in the electroweak unified theory*, *Lett. Nuovo Cim.* **38** (1983) 593 [INSPIRE].
- [22] J.C. Montero, V. Pleitez and M.C. Rodriguez, *Left-right asymmetries in polarized e - mu scattering*, *Phys. Rev. D* **58** (1998) 097505 [[hep-ph/9803450](#)] [INSPIRE].
- [23] T. Gehrmann and E. Remiddi, *Two loop master integrals for $\gamma \rightarrow 3$ jets: the nonplanar topologies*, *Nucl. Phys. B* **601** (2001) 287 [[hep-ph/0101124](#)] [INSPIRE].
- [24] R. Bonciani, P. Mastrolia and E. Remiddi, *Master integrals for the two loop QCD virtual corrections to the forward backward asymmetry*, *Nucl. Phys. B* **690** (2004) 138 [[hep-ph/0311145](#)] [INSPIRE].
- [25] R. Bonciani and A. Ferroglia, *Two-Loop QCD Corrections to the Heavy-to-Light Quark Decay*, *JHEP* **11** (2008) 065 [[arXiv:0809.4687](#)] [INSPIRE].
- [26] H.M. Asatrian, C. Greub and B.D. Pecjak, *NNLO corrections to $\bar{B} \rightarrow X_u \ell \bar{\nu}$ in the shape-function region*, *Phys. Rev. D* **78** (2008) 114028 [[arXiv:0810.0987](#)] [INSPIRE].
- [27] M. Beneke, T. Huber and X.Q. Li, *Two-loop QCD correction to differential semi-leptonic $b \rightarrow u$ decays in the shape-function region*, *Nucl. Phys. B* **811** (2009) 77 [[arXiv:0810.1230](#)] [INSPIRE].
- [28] G. Bell, *NNLO corrections to inclusive semileptonic B decays in the shape-function region*, *Nucl. Phys. B* **812** (2009) 264 [[arXiv:0810.5695](#)] [INSPIRE].
- [29] T. Huber, *On a two-loop crossed six-line master integral with two massive lines*, *JHEP* **03** (2009) 024 [[arXiv:0901.2133](#)] [INSPIRE].
- [30] R. Bonciani, A. Ferroglia, T. Gehrmann, D. Maître and C. Studerus, *Two-loop fermionic corrections to heavy-quark pair production: the quark-antiquark channel*, *JHEP* **07** (2008) 129 [[arXiv:0806.2301](#)] [INSPIRE].
- [31] R. Bonciani, A. Ferroglia, T. Gehrmann and C. Studerus, *Two-loop planar corrections to heavy-quark pair production in the quark-antiquark channel*, *JHEP* **08** (2009) 067 [[arXiv:0906.3671](#)] [INSPIRE].
- [32] R. Bonciani, A. Ferroglia, T. Gehrmann, A. von Manteuffel and C. Studerus, *Two-loop leading color corrections to heavy-quark pair production in the gluon fusion channel*, *JHEP* **01** (2011) 102 [[arXiv:1011.6661](#)] [INSPIRE].
- [33] R. Bonciani et al., *Light-quark two-loop corrections to heavy-quark pair production in the gluon fusion channel*, *JHEP* **12** (2013) 038 [[arXiv:1309.4450](#)] [INSPIRE].
- [34] F.V. Tkachov, *A theorem on analytical calculability of four loop renormalization group functions*, *Phys. Lett. B* **100** (1981) 65.
- [35] K.G. Chetyrkin and F.V. Tkachov, *Integration by parts: the algorithm to calculate β -functions in 4 loops*, *Nucl. Phys. B* **192** (1981) 159 [INSPIRE].

- [36] S. Laporta, *High precision calculation of multiloop Feynman integrals by difference equations*, *Int. J. Mod. Phys. A* **15** (2000) 5087 [[hep-ph/0102033](#)] [[INSPIRE](#)].
- [37] A.V. Kotikov, *Differential equations method: new technique for massive Feynman diagrams calculation*, *Phys. Lett. B* **254** (1991) 158 [[INSPIRE](#)].
- [38] E. Remiddi, *Differential equations for Feynman graph amplitudes*, *Nuovo Cim. A* **110** (1997) 1435 [[hep-th/9711188](#)] [[INSPIRE](#)].
- [39] T. Gehrmann and E. Remiddi, *Differential equations for two loop four point functions*, *Nucl. Phys. B* **580** (2000) 485 [[hep-ph/9912329](#)] [[INSPIRE](#)].
- [40] J.M. Henn, *Multiloop integrals in dimensional regularization made simple*, *Phys. Rev. Lett.* **110** (2013) 251601 [[arXiv:1304.1806](#)] [[INSPIRE](#)].
- [41] M. Argeri et al., *Magnus and Dyson series for master integrals*, *JHEP* **03** (2014) 082 [[arXiv:1401.2979](#)] [[INSPIRE](#)].
- [42] S. Di Vita, P. Mastrolia, U. Schubert and V. Yundin, *Three-loop master integrals for ladder-box diagrams with one massive leg*, *JHEP* **09** (2014) 148 [[arXiv:1408.3107](#)] [[INSPIRE](#)].
- [43] R. Bonciani, S. Di Vita, P. Mastrolia and U. Schubert, *Two-loop master integrals for the mixed EW-QCD virtual corrections to Drell-Yan scattering*, *JHEP* **09** (2016) 091 [[arXiv:1604.08581](#)] [[INSPIRE](#)].
- [44] S. Di Vita, P. Mastrolia, A. Primo and U. Schubert, *Two-loop master integrals for the leading QCD corrections to the Higgs coupling to a W pair and to the triple gauge couplings ZWW and γ^*WW* , *JHEP* **04** (2017) 008 [[arXiv:1702.07331](#)] [[INSPIRE](#)].
- [45] A. Goncharov, *Polylogarithms in arithmetic and geometry*, *Proc. Int. Congress Math.* **1,2** (1995) 374.
- [46] E. Remiddi and J.A.M. Vermaseren, *Harmonic polylogarithms*, *Int. J. Mod. Phys. A* **15** (2000) 725 [[hep-ph/9905237](#)] [[INSPIRE](#)].
- [47] T. Gehrmann and E. Remiddi, *Numerical evaluation of harmonic polylogarithms*, *Comput. Phys. Commun.* **141** (2001) 296 [[hep-ph/0107173](#)] [[INSPIRE](#)].
- [48] J. Vollinga and S. Weinzierl, *Numerical evaluation of multiple polylogarithms*, *Comput. Phys. Commun.* **167** (2005) 177 [[hep-ph/0410259](#)] [[INSPIRE](#)].
- [49] C.W. Bauer, A. Frink and R. Kreckel, *Introduction to the GiNaC framework for symbolic computation within the C++ programming language*, [cs/0004015](#).
- [50] S. Borowka et al., *SecDec-3.0: numerical evaluation of multi-scale integrals beyond one loop*, *Comput. Phys. Commun.* **196** (2015) 470 [[arXiv:1502.06595](#)] [[INSPIRE](#)].
- [51] A. von Manteuffel and C. Studerus, *Reduze 2 — Distributed Feynman Integral Reduction*, [arXiv:1201.4330](#) [[INSPIRE](#)].
- [52] V.A. Smirnov, *Analytical result for dimensionally regularized massless on shell double box*, *Phys. Lett. B* **460** (1999) 397 [[hep-ph/9905323](#)] [[INSPIRE](#)].
- [53] J.B. Tausk, *Nonplanar massless two loop Feynman diagrams with four on-shell legs*, *Phys. Lett. B* **469** (1999) 225 [[hep-ph/9909506](#)] [[INSPIRE](#)].
- [54] M. Czakon, *Tops from light quarks: full mass dependence at two-loops in QCD*, *Phys. Lett. B* **664** (2008) 307 [[arXiv:0803.1400](#)] [[INSPIRE](#)].

- [55] M. Czakon and A. Mitov, *NNLO corrections to top pair production at hadron colliders: the quark-gluon reaction*, *JHEP* **01** (2013) 080 [[arXiv:1210.6832](#)] [[INSPIRE](#)].
- [56] M. Czakon and A. Mitov, *NNLO corrections to top-pair production at hadron colliders: the all-fermionic scattering channels*, *JHEP* **12** (2012) 054 [[arXiv:1207.0236](#)] [[INSPIRE](#)].
- [57] P. Bärnreuther, M. Czakon and A. Mitov, *Percent level precision physics at the Tevatron: first genuine NNLO QCD corrections to $q\bar{q} \rightarrow t\bar{t} + X$* , *Phys. Rev. Lett.* **109** (2012) 132001 [[arXiv:1204.5201](#)] [[INSPIRE](#)].
- [58] M. Czakon, P. Fiedler and A. Mitov, *Total top-quark pair-production cross section at hadron colliders through $O(\alpha_S^4)$* , *Phys. Rev. Lett.* **110** (2013) 252004 [[arXiv:1303.6254](#)] [[INSPIRE](#)].
- [59] E. Remiddi and L. Tancredi, *Differential equations and dispersion relations for Feynman amplitudes. The two-loop massive sunrise and the kite integral*, *Nucl. Phys. B* **907** (2016) 400 [[arXiv:1602.01481](#)] [[INSPIRE](#)].
- [60] A. Primo and L. Tancredi, *On the maximal cut of Feynman integrals and the solution of their differential equations*, *Nucl. Phys. B* **916** (2017) 94 [[arXiv:1610.08397](#)] [[INSPIRE](#)].
- [61] A. Primo and L. Tancredi, *Maximal cuts and differential equations for Feynman integrals. An application to the three-loop massive banana graph*, *Nucl. Phys. B* **921** (2017) 316 [[arXiv:1704.05465](#)] [[INSPIRE](#)].
- [62] F. Brown, *On the decomposition of motivic multiple zeta values*, [arXiv:1102.1310](#) [[INSPIRE](#)].
- [63] C. Duhr, *Hopf algebras, coproducts and symbols: an application to Higgs boson amplitudes*, *JHEP* **08** (2012) 043 [[arXiv:1203.0454](#)] [[INSPIRE](#)].
- [64] C. Duhr, *Mathematical aspects of scattering amplitudes*, in the proceedings of the *Theoretical Advanced Study Institute in Elementary Particle Physics (TASI 2014)*, June 2–27, Boulder, Colorado, U.S.A. (2014) [arXiv:1411.7538](#) [[INSPIRE](#)].
- [65] D.J. Broadhurst, *Massive three-loop Feynman diagrams reducible to SC^* primitives of algebras of the sixth root of unity*, *Eur. Phys. J. C* **8** (1999) 311 [[hep-th/9803091](#)] [[INSPIRE](#)].
- [66] J. Zhao, *Standard relations of multiple polylogarithm values at roots of unity*, [arXiv:0707.1459](#).
- [67] J.M. Henn, A.V. Smirnov and V.A. Smirnov, *Evaluating multiple polylogarithm values at sixth roots of unity up to weight six*, *Nucl. Phys. B* **919** (2017) 315 [[arXiv:1512.08389](#)] [[INSPIRE](#)].
- [68] F. Dulat and B. Mistlberger, *Real-Virtual-Virtual contributions to the inclusive Higgs cross section at N3LO*, [arXiv:1411.3586](#) [[INSPIRE](#)].